1-1-2004

An improved multiscale model for dilute turbulent gas particle flows based on the equilibration of energy concept

Ying Xu
Iowa State University

An improved multiscale model for dilute turbulent gas particle flows based on the equilibration of energy concept

by

Ying Xu

A thesis submitted to the graduate faculty

in partial fulfillment of the requirements for the degree of

MASTER OF SCIENCE

Major: Mechanical Engineering

Program of Study Committee:
Shankar Subramaniam, Major Professor
Francine Battaglia
James C. Hill

Iowa State University

Ames, Iowa

2004

Graduate College
Iowa State University

This is to certify that the master's thesis of

Ying Xu

has met the thesis requirements of Iowa State University

Signatures have been redacted for privacy

TABLE OF CONTENTS

LIST OF TABLES

LIST OF FIGURES

NOMENCLATURE

b_j	body force in j^{th} direction
$\bar{d}$	the mean particle diameter
e_c	restitution coefficience
I_β	indicator function of β^{th} phase
k	turbulence kinetic energy
k_{fp}	covariance of fluid–particle velocity in Simonin's model
Re_p	particle Reynolds number
p_β	probability of β^{th} phase at $(\mathbf{x}, t)$
$R_{ij}^{(\beta)}$	Reynolds stress in β^{th} phase
S	mean velocity shear rate in particle-laden homogeneous shear flows
$S_{Mj}^{(\beta)}$	interphase momentum transfer source in β^{th} phase
$S_\rho^{(\beta)}$	interfical mass transfer rate
St	particle Stokes number (based on Kolmogorov length scale)
t	time
T_L	Lagrangian time macroscale of fluid turbulence in Ahmadi's model
$\langle \tilde{U}_k^{(\beta)} \rangle$	unconditional density-weighted mean-velocity in β^{th} phase
$\langle \tilde{U}_k^{(m)} \rangle$	unconditional density–weighted mean mixture velocity
$\langle U_k^{(\beta)} \rangle$	unconditional mean velocity in β^{th} phase without density–weighting
$\langle U_k^{(m)} \rangle$	unconditional mean mixture velocity without density-weighting
$U^{(I)}$	interface velocity
x_1	direction of the mean flow velocity in particle-laden homogeneous shear flows
x_3	direction of the mean flow velocity shear in particle-laden homogeneous shear flows

Greek Symbols

α	volume fraction
ε_f	turbulent dissipation rate in fluid phase
ν_T	turbulent eddy viscosity
μ_f^T	turbulent eddy viscosity in fluid phase
μ_p^T	turbulent eddy viscosity in particle phase
σ_k	turbulent Prandtl number for kinetic energy
Π_{k_f}	interphase turbulence kinetic energy transfer term for k_f equation
Π_{k_p}	interphase turbulence kinetic energy transfer term for k_p equation
Π_{ε_f}	interphase turbulence kinetic energy transfer term for ε_f equation
$\Pi_{k_{fp}}$	interphase turbulence kinetic energy transfer term for k_{fp} equation
ϕ	mass loading ratio
ρ	density
$\rho_{f1,3}$	correlation of fluid fluctuating velocity in x_1 and x_3 direction
τ_{ij}	stress tensor
τ_{12}^F	particle response time in Simonin's model
τ_{12}^t	time scale of fluid turbulent motion viewed by the particles in Simonin's model
τ_i	multiscale interaction time scale
τ_l	characteristic eddy time scale
τ	eddy turnover time
τ_η	Kolmogorov length scale
ξ	particle radial distribution function

Superscripts

(p)	particle phase
(f)	fluid phase

$'$	fluctuating component of variable

Subscripts

f	fluid phase
p	particle phase

Other Symbols

$\langle\rangle$	mean or expectation

Abbreviations

CFD	computational fluid dynamics
DNS	direct numerical simulations
PDF	probability density functiom
RANS	Reynolds–averaged Navier–Stokes equations

ABSTRACT

Many particle–laden flows in engineering applications involve turbulent gas flows. Modeling multiphase turbulent flows is an important research topic with applications in fluidized beds and particle conveying. A predictive multiphase turbulence model can help CFD codes to be more useful for engineering applications, such as the scale–up in the design of circulating fluidized combustor and coal gasifications.

In engineering applications, the particle volume fraction can vary from dilute ($< 10^{-4}$) to dense ($\sim 50\%$). It is reasonable to expect that multiphase turbulence models should at least satisfy some basic modeling and performance criteria and give reasonable predictions for the canonical problems in dilute particle–laden turbulent flows.

In this research, a comparative assessment of predictions from Simonin and Ahmadi's turbulence models is performed with direct numerical simulation (DNS) for two canonical problems in particle–laden turbulent flows. Based on the comparative assessment, some criteria and the areas for model improvement are identified: (i) model for interphase TKE transfer, especially the time scale of interphase TKE transfer, and (ii) correct prediction of TKE evolution with variation of particle Stokes number. Some deficiencies that are identified in the Simonin and Ahmadi models, limit the applicability.

A new multiphase turbulence model, the Equilibration of Energy Model (EEM), is proposed in this work. In EEM, a multiscale interaction time scale is proposed to account for the interaction of a particle with a range of eddy sizes. EEM shows good agreement with the DNS results for particle–laden isotropic turbulence. For particle–laden homogeneous shear flows, model predictions from EEM can be further improved if the dissipation rate in fluid phase is modeled with more accuracy.

This new time scale is incorporated in the interphase TKE transfer terms of the Simonin and Ahmadi models. For canonical problems in particle–laden turbulent flows, this time scale improves the predictions from these two models.

Although EEM is a simple model, it has clear a physical interpretation and gives reasonable predictions for two canonical problems in particle–laden turbulent flows. It can be a useful engineering tool for CFD calculations of gas–solid two phase flows.

CHAPTER 1. INTRODUCTION

1.1 Background

Modeling turbulent particle-laden flows is an important research topic with applications in fluidized beds and particle transport through pneumatic conveying. In applications like fluidized beds, the particle volume fraction varies tremendously, from very dense-packed beds($>$ 0.4) to dilute two phase flow at the top of a circulating fluidized bed (< 0.001). Two distinct regimes of particle-laden flows can be found in fluidized bed. One includes solid suspensions that are low in volume fraction, but still have relatively high mass loading, due to high thermodynamic particle density. Since this particle volume fraction is low, the influence of particle on the carrier phase mass conservation equation is often neglected, and so is the inter–particle collisions. Recently analyses show that the former assumption is not entirely justified. However the particles greatly alter the turbulence in the carrier phase, hence the "two-way" coupling should be taken into consideration. The other regime is high in both particle volume fraction and mass loading, and the influence of dispersed phase or particles on the continuity equation of the carrier or fluid phase cannot be ignored. At high particle volume concentrations, particle dynamics become collision-dominated. In this work, we mainly focus on the particle suspensions that are volumetric dilute, but still have moderately high mass loading.

Many dilute particle-laden flows in engineering applications involve turbulent gas flows. Turbulence enhances the momentum, heat and mass transfer between the dispersed phase and the carrier phase. It is useful to adopt a statistical description in these flows. Two commonly used modeling approaches to describe two-phase turbulent flows are the two-fluid (or Eulerian–Eulerian approach), and the number-density based Lagrangian–Eulerian approach [2, 3]. In the Lagrangian–Eulerian approach, Reynolds–averaged Navier-Stokes equations are

used to solve the fluid phase, while the dispersed phase is modeled by tracking the motion of Lagrangian particles. In the Eulerian–Eulerian approach, the multiphase flow quantities like velocity and volume fraction in each phase are averaged, and these averaged quantities are used to describe the characteristics of the flow field. The nature of this approach leads to unclosed terms representing the interaction between the phases. Once these terms are modeled to close the equation system, the Eulerian–Eulerian approach can be used widely in multiphase flow simulations. The focus is on Eulerian–Eulerian approach in this thesis.

Some popular multiphase turbulence models are reviewed here, which are based on the Eulerian–Eulerian approach. Elghobashi [4] developed a two–equation turbulence model, which describes the conservation of turbulent kinetic energy (TKE) and dissipation rate in the fluid phase based on the volume averaging method. This two phase $k-\varepsilon$ model was validated by comparing with results from particle-laden jet flow [5] and jet flows laden with vaporizing droplets [6]. The volume averaging approach is used in this model, and it could cause problems if this model is used in a spatially inhomogeneous turbulent flow.

Ahmadi [7] used the ensemble averaging method to derive the conservation laws for TKE in the carrier and dispersed phases. Two transport equations are derived for the evolution of TKE in both phases, and an algebraic model is applied in the dissipation rate of the fluid energy. The model contains the specification for dilute two-phase flows and dense granular flows as special limiting cases. Validation of this model has been reported in the simple shear flow for dense mixture [8] and gas-particle turbulent flows in a vertical duct [9]. In Ahmadi's model, the length scale used in fluid phase dissipation is not a self-contained term and needs further specification when using it.

A four-equation model proposed by Simonin and co-workers [10, 11, 12, 13] has been tested by other researchers [14] and compared with experimental results for the turbulent gas-solid flows in a vertical pipe [15], and in a vertical riser [16]. Based on this model, a single phase $k-\varepsilon$ model is added in MFIX (Multiphase **F**low with **I**nterphase e**X**changes) kernel and a turbulent pipe flow test case is included in latest version of MFIX.

MFIX is a general–purpose hydrodynamic model for describing chemical reactions and heat

transfer in dense or dilute fluid-solid flows [17], and it is based on a two-fluid modeling approach [18] for multiphase flows. There are other CFD codes developed for describing the flow field and heat transfer in the dilute and dense fluid-solid flows in fluidization and particle transport in pneumatic conveying. A detailed list of this group of CFD codes can be found in Peirano's review of Eulerian two–phase flow theory for fluidization [19]. It includes MFIX, MELODIF, and GEMINI from Enwald's group [19] to name a few. MFIX is now maintained and developed by EG&G W.A.S.C. Inc./Department of Energy Morgantown group. MELODIF is developed by Electricité de France(EDF) group, which made quite detailed analysis of the two-fluid model and constitutive equations applied to gas-particle fluidization. Simonin's multiphase turbulence model is tested in MELODIF.

These CFD codes can be useful for engineering application, such as the scale-up in the design of circulating fluidized combustor, and coal gasification, only if the turbulence models are predictive. The turbulence model should satisfy some basic modeling and performance criteria. These criteria could be found in Direct Numerical Simulations (DNS) data and experiments for gas-solid turbulent flows. Furthermore, the multiphase turbulence model should give reasonable predictions for canonical problems in particle–laden turbulent flows. By identifying these criteria, CFD calculations in the general code like MFIX, can be further improved.

1.2 Statement of Problem

The objective of this work is to:

(1) perform a comparative assessment of model predictions with direct numerical simulation data for the canonical problems in particle–laden turbulent flows,

(2) identify the modeling criteria based on comparative assessment,

(3) propose a new multiphase turbulence model for dilute particle–laden turbulent flows, which satisfies the modeling criteria in comparative assessment.

The thesis is organized as follows. The governing equations for gas-solid two phase turbulent flows in the Eulerian–Eulerian approach are discussed in Chapter 2. Chapter 3 describes the

canonical test problems. One is particle-laden isotropic decaying turbulent flows for which DNS was performed by Sundaram and Collins [1], and the other is the homogeneous shear flows laden with particles for which DNS was performed by Elghobashi [20]. In Chapter 4, two multiphase turbulence models due to Simonin [10, 11] and Ahmadi [7, 8] are discussed. Some numerical issues encountered in solving these model equations are also discussed in this chapter. The comparative assessment of model results with DNS data for the particle-laden isotropic turbulent flow and the homogeneous shear flow is discussed in Chapter 5.

A new multiphase model, the Equilibration of Energy Model (EEM), is proposed in Chapter 6. Since turbulence has various length and time scales, a multiscale interaction time scale for interphase TKE transfer is used in EEM. In fact, incorporating the EEM specification for the interphase TKE transfer time scale improves the performance of the two multiphase turbulence models. The model predictions from EEM for canonical test problems are discussed in Chapter 6. The conclusions of this study and recommendations for future work are discussed in Chapter 7.

CHAPTER 2. SYSTEM OF EQUATIONS IN EULERIAN-EULERIAN FORMULATION FOR MULTIPHASE TURBULENT FLOWS

The Eulerian–Eulerian (EE) or two–fluid approach is one of the statistical models for two–phase flow that is used in CFD calculations of multiphase flows. There are several ways of defining averaged equations in Eulerian–Eulerian approach, and one may use temporal or volume averaging. Time averaging is strictly applicable to only statistically stationary flows, while volume averaging is strictly applicable only to statistically homogeneous flows. Drew's formulation [21] of two–phase flow problem uses the ensemble–averaging which enables the Eulerian–Eulerian approach to be applied to statistically unsteady, inhomogeneous problems. In this chapter, the governing equations for first and second moments of velocity [2, 3] are derived following Drew's formulation.

2.1 Random–Field Representation of Two–Phase Flow

Consider a gas–solid two–phase flow, the dispersed phase is rigid solid particles and then each particle has constant thermodynamics density. Let $I_\beta(\mathbf{x}, t)$ donate the indicator function of the βth phase, which is unity if the location $\mathbf{x}$ in physical space is occupied by phase β at time t, and zero otherwise. It is assumed that (i) the density difference between the two phases is sufficiently large so that the density field can be used to distinguish between the two phases, and (ii) the characteristic length scale of the interface over which this density change occurs is so small that in a continuum description the density changes discontinuously at the interface. The second assumption implies that in two-phase flows the phase indicator functions satisfy the relation

$$\sum_{\beta=1}^{2} I_\beta(\mathbf{x}, t) = 1 \tag{2.1}$$

for all $(\mathbf{x}, t)$. The phase index is β and the particle phase is referred to as $\beta = p$ and the fluid or carrier phase as $\beta = f$.

The event associated with the random-field representation is $E_0^{(\beta)} = [I_\beta(\mathbf{x}, t) = 1]$. The probability of this event defines a probability field $\alpha_\beta(\mathbf{x}, t)$:

$$\alpha_\beta(\mathbf{x}, t) \equiv P[I_\beta(\mathbf{x}, t) = 1]. \tag{2.2}$$

It is important to note that $\alpha_\beta(\mathbf{x}, t)$ is *not* a probability density in $\mathbf{x}$, because the sample space of $I_\beta(\mathbf{x}, t)$ is $\{0, 1\}$. For two-phase flows the p_β satisfy the relation

$$\sum_{\beta=1}^{2} \alpha_\beta(\mathbf{x}, t) = 1, \tag{2.3}$$

In the Eulerian–Eulerian formulation for two–phase flow fields, phasic average or phase–average fields are used to describe the two–phase flows [21]. The phasic average is a conditional average, where the average is conditional on the even $E_0^{(\beta)}$, i.e., on the presence of phase β at that space–time location $(\mathbf{x}, t)$. In particular, the mean density and velocity field *conditional* on the presence of phase β is used in the formulation. The mean density conditional on phase β is defined as

$$\langle \rho^\beta(\mathbf{x}, t) \rangle \equiv \langle \rho | I_\beta = 1 \rangle \equiv \frac{\langle \rho(\mathbf{x}, t) I_\beta(\mathbf{x}, t) \rangle}{\langle I_\beta(\mathbf{x}, t) \rangle} \tag{2.4}$$

Using standard conditioning arguments of probability it is easy to show that the expected value of the indicator function $I_\beta(\mathbf{x}, t)$ that appears in the denominator of Eq. 2.4 is simply the probability field $p_\beta(\mathbf{x}, t)$:

$$\langle I_\beta(\mathbf{x}, t) \rangle = \sum_{\gamma=1}^{2} \langle I_\beta | I_\gamma = 1 \rangle \alpha_\gamma(\mathbf{x}, t) = \alpha_\beta(\mathbf{x}, t) \tag{2.5}$$

The unconditional mean density field of the two–phase mixture $\langle \rho(\mathbf{x}, t) \rangle$ is defined as

Since we consider two-phase flows with constant thermodynamic density, $\langle \rho(\mathbf{x}, t) I_\beta(\mathbf{x}, t) \rangle$ is completely determined by the phase probability field such that

$$\langle \rho(\mathbf{x}, t) I_\beta(\mathbf{x}, t) \rangle = \rho_\beta \cdot \alpha_\beta(\mathbf{x}, t) \tag{2.6}$$

The mean velocity field can be defined in terms of conditional *density-weighted* average:

$$\langle \tilde{U}_k^{(\beta)} \rangle \equiv \frac{\langle \rho I_\beta U_k \rangle}{\langle \rho I_\beta \rangle} \tag{2.7}$$

These *density-weighted* averages are the most convenient description of the mean velocity fields in the mean momentum equations. The mean velocity conditioned on phase β without density-weighting is defined as:

$$\langle U_k^{(\beta)} \rangle \equiv \frac{\langle I_\beta U_k \rangle}{\langle I_\beta \rangle} \tag{2.8}$$

For the constant density two-phase flows ($\langle \rho | I_\beta = 1 \rangle = \rho_\beta$), the *conditional density-weighted* mean velocity fields are identical to their unweighted conditional mean velocity:

$$\langle \tilde{U}_k^{(\beta)} \rangle \equiv \frac{\langle \rho I_\beta U_k \rangle}{\langle \rho I_\beta \rangle} = \frac{\langle I_\beta U_k \rangle}{\langle I_\beta \rangle} \equiv \langle U_k^{(\beta)} \rangle. \tag{2.9}$$

The unconditional *density-weighted* mean velocity field of the mixture $\langle \tilde{\mathbf{U}}^{(m)}(\mathbf{x},t) \rangle = \langle \rho \mathbf{U} \rangle / \langle \rho \rangle$ is defined as

$$\langle \tilde{\mathbf{U}}^{(m)} \rangle = \frac{1}{\langle \rho \rangle} \sum_{\beta=1}^{2} \langle \rho^{(\beta)} \rangle \langle \tilde{\mathbf{U}}^{(\beta)} \rangle \tag{2.10}$$

This unconditional *density-weighted* mean mixture velocity field $\langle \tilde{\mathbf{U}}^{(\beta)}(\mathbf{x},t) \rangle$ in multiphase flow is analogous to the Favre-averaged velocity in variable-density single-phase turbulent reacting flows.

The unconditional mean velocity without density-weighting can be recovered from $\{ \langle U_k^{(\beta)} \rangle, \beta = 1,2 \}$ using the relation

$$\langle \mathbf{U}^{(m)} \rangle = \sum_{\beta=1}^{2} \alpha_\beta \langle \mathbf{U}^\beta \rangle \tag{2.11}$$

It is easy to show that in multiphase flows $\langle \tilde{\mathbf{U}}^{(m)} \rangle \neq \langle \mathbf{U}^{(m)} \rangle$ even for the constant-density case, because of the different weighting factors in Eqs. 2.10 and 2.11.

2.2 Equation System in Eulerian–Eulerian Approach

In Drew's formulation, the governing equations for mean mass and momentum equation are derived by multiplying the standard Navier–Stokes equations by the indicator function $I_\beta(\mathbf{x},t)$ and taking expectations of the resulting equations. Here $I_\beta(\mathbf{x},t)$ is a Heaviside function which has the special properties of generalized functions. This procedure follows Drew's exposition of the mathematical theory of two–phase flows.

Mean Mass Conservation

The mean mass conservation in each phase ($\beta = f, p$) is:

$$\frac{\partial}{\partial t}[\alpha_\beta \langle \rho | I_\beta = 1 \rangle] + \frac{\partial}{\partial x_k}[\alpha_\beta \langle \rho | I_\beta = 1 \rangle \langle \tilde{U}_k^{(\beta)} \rangle] = \langle S_\rho^{(\beta)} \rangle. \tag{2.12}$$

where the source term on the right-hand-side of Eq. 2.12 is given by

$$\langle S_\rho^{(\beta)} \rangle = \left\langle \rho \left(U_i - U_i^{(I)} \right) \frac{\partial I_\beta}{\partial x_i} \right\rangle \tag{2.13}$$

and $U_i^{(I)}$ is the velocity of the interface.

Taking the expectations of the instantaneous mass conservation equation, and summing over both phases gives the constraint

$$\langle S_\rho^{(\beta=f)} \rangle = -\langle S_\rho^{(\beta=p)} \rangle. \tag{2.14}$$

For zero interphase mass transfer, such as gas-solid flows, the source term $\langle S_\rho^{(\beta)} \rangle$ is zero.

Mean Momentum Equation

The mean momentum conservation in each phase ($\beta = f, p$) is:

$$\begin{aligned} &\frac{\partial}{\partial t}[\alpha_\beta \langle \rho | I_\beta = 1 \rangle \langle \tilde{U}_j^{(\beta)} \rangle] + \frac{\partial}{\partial x_k}[\alpha_\beta \langle \rho | I_\beta = 1 \rangle \langle \tilde{U}_j^{(\beta)} \rangle \langle \tilde{U}_k^{(\beta)} \rangle] \\ &= -\frac{\partial}{\partial x_i}[\alpha_\beta \langle \rho | I_\beta = 1 \rangle \tilde{R}_{ij}^{(\beta)}] + \frac{\partial}{\partial x_i} \langle I_\beta \tau_{ij} \rangle + \langle I_\beta \rho b_j \rangle + \langle S_{Mj}^{(\beta)} \rangle \end{aligned} \tag{2.15}$$

where $\tilde{R}_{ij}^{(\beta)}$ is the Reynolds stress in phase β, the definition of which will be discussed later in this chapter; $\langle I_\beta \tau_{ij} \rangle$ is the expected stress tensor weighted by the phase indicator function; $\langle I_\beta \rho b_j \rangle$ is the expected body force weighted by the phase indicator function, and $\langle S_{Mj}^{(\beta)} \rangle$ is the interphase momentum transfer source in β phase,

$$\langle S_{Mj}^{(\beta)} \rangle = \left\langle \rho U_j \left(U_i - U_i^{(I)} \right) \frac{\partial I_\beta}{\partial x_i} - \tau_{ij} \frac{\partial I_\beta}{\partial x_i} \right\rangle \tag{2.16}$$

The interphase momentum transfer source has two parts: the first term represents the contributions from the interphase mass transfer, while the second term is due to the fact that the interface can support a stress difference. For gas–solid two–phase flows, the first term in

$\langle S_{Mj}^{(\beta)} \rangle$ is zero, and the second term is required for closure through modeling. The interphase momentum source is subject to the following constraint

$$\langle \mathbf{S}_M^{(\beta=f)} \rangle = -\langle \mathbf{S}_M^{(\beta=p)} \rangle + \langle \mathbf{M}^{(I)} \rangle \tag{2.17}$$

where $\langle \mathbf{M}^{(I)} \rangle$ is the average momentum associated with the interface. When the dispersed–phase is a solid, the average momentum associated with the interface $\langle \mathbf{M}^{(I)} \rangle$ is zero. In this work, we are concerned with isothermal constant–density two–phase flows, and therefore an equation of state and energy equation are not required for closure.

2.3 Second Moment Equations

The evolution equations for the second moment of velocity based on Eulerian–Eulerian approach are presented in this section. Before describing the second–moment evolution equations for velocity, the fluctuating velocity field needs to be defined. The fluctuating velocity in phase β is defined as

$$u_i''^{(\beta)} \equiv U_i - \langle \tilde{U}_i^{(\beta)} \rangle \tag{2.18}$$

where U_i is the velocity field, and $\langle \tilde{U}_i^{(\beta)} \rangle$ is the conditional *density–weighted* average defined as

$$\langle \tilde{U}_i^{(\beta)} \rangle \equiv \frac{\langle \rho I_\beta U_i \rangle}{\langle \rho I_\beta \rangle} \tag{2.19}$$

where I_β is the phase indicator function of the βth phase. Based on the definition of (density-weighted) fluctuating velocity, the Reynolds stress $\tilde{R}_{ij}^{(\beta)}$ is defined as

$$\tilde{R}_{ij}^{(\beta)} \equiv \frac{\left\langle I_\beta \rho u_i''^{(\beta)} u_j''^{(\beta)} \right\rangle}{\langle I_\beta \rho \rangle} \tag{2.20}$$

For gas-solid two-phase flows, without interphase mass transfer, the evolution equation of

the Reynolds stress $\tilde{R}_{ij}^{(\beta)}$ in phase β is

$$\begin{aligned}
&\langle I_\beta \rho \rangle \frac{\tilde{D}_\beta}{\tilde{D}_\beta t} \tilde{R}_{ij}^{(\beta)} + \frac{\partial}{\partial x_k} \left\langle I_\beta \rho u_i^{\prime\prime(\beta)} u_j^{\prime\prime(\beta)} u_k^{\prime\prime(\beta)} \right\rangle = \\
&- \left\{ \left\langle I_\beta \rho u_i^{\prime\prime(\beta)} u_k^{\prime\prime(\beta)} \right\rangle \frac{\partial \left\langle \tilde{U}_j^{(\beta)} \right\rangle}{\partial x_k} \right\} - \left\{ \left\langle I_\beta \rho u_j^{\prime\prime(\beta)} u_k^{\prime\prime(\beta)} \right\rangle \frac{\partial \left\langle \tilde{U}_i^{(\beta)} \right\rangle}{\partial x_k} \right\} \\
&+ \left\langle u_i^{\prime\prime(\beta)} \frac{\partial (I_\beta \tau_{kj})}{\partial x_k} \right\rangle + \left\langle u_j^{\prime\prime(\beta)} \frac{\partial (I_\beta \tau_{ki})}{\partial x_k} \right\rangle \\
&+ \left\langle u_i^{\prime\prime(\beta)} S_{Mj}^{(\beta)} \right\rangle + \left\langle u_j^{\prime\prime(\beta)} S_{Mi}^{(\beta)} \right\rangle
\end{aligned} \tag{2.21}$$

where the terms on the left hand side are:

(i) the material derivative of the Reynolds stress in phase β with the density-weighted mean velocity in phase β,

(ii) the triple velocity correlation term.

The terms on the right hand side are:

(iii)-(iv) production of Reynolds stress due to the mean velocity gradients,

(v)-(vi) fluctuating velocity-stress gradient correlation,

(vii)-(viii) fluctuating velocity-interfacial momentum transfer correlation.

In Eq. 2.21 $S_{Mj}^{(\beta)}$ is the interphase momentum transfer source term in phase β.

The material derivative moving with the density–weighted mean velocity in phase β is defined as:

$$\frac{\tilde{D}_\beta}{\tilde{D}_\beta t} = \frac{\partial}{\partial t} + \left\langle \tilde{U}_k^{(\beta)} \right\rangle \frac{\partial}{\partial x_k} \tag{2.22}$$

The kinetic energy k_f and k_p in the fluid and particle (or dispersed) phase respectively, are the half of the trace of the Reynolds stress tensor. For gas–solid two–phase flows, the thermodynamic density is constant in each phase and the dispersed phase is rigid particle. Furthermore, the unconditional *density–weighted* mean velocity is equal to the mean velocity *without density–weighting*. The evolution equation for kinetic energy in phase β can be

simplified from Eq. 2.21 as

$$\alpha_\beta \rho_\beta \frac{\partial k_\beta}{\partial t} + \tilde{U}_k^{(\beta)} \alpha_\beta \rho_\beta \frac{\partial k_\beta}{\partial x_k} + \frac{1}{2} \alpha_\beta \rho_\beta \frac{\partial}{\partial x_k} \left\langle u_i''^{(\beta)} u_i''^{(\beta)} u_k''^{(\beta)} \right\rangle =$$
$$- \left\{ \left\langle I_\beta \rho u_i''^{(\beta)} u_k''^{(\beta)} \right\rangle \frac{\partial \langle \tilde{U}_i^{(\beta)} \rangle}{\partial x_k} \right\} + \left\langle u_i''^{(\beta)} \frac{\partial (I_\beta \tau_{ki})}{\partial x_k} \right\rangle + \left\langle u_i''^{(\beta)} S_{Mj}^{(\beta)} \right\rangle \qquad (2.23)$$

where α_β is defined in Eq. 2.2, which is the probability of phase β appearing in the physical space $\mathbf{x}$. ρ_β is the density in phase β. The third term on the left hand side is the triple velocity correlation term. The terms on the right hand side are

(i) the production of TKE in phase β due to the mean velocity gradient,

(ii) the fluctuating velocity–stress gradient and fluctuating velocity–pressure correlation, where the contribution from pressure correlation is neglected, and this term is modeled as the dissipation in the phase β;

(iii) the fluctuating velocity–interfacial momentum transfer correlation.

The third term is not in the second moment equations for the single phase turbulence. It is this term that place the challenge on modeling rather than the other two terms on right side of Eq. 2.23, and is called interphase TKE transfer in the later chapters.

Two canonical cases for particle–laden turbulent flows will be described in the next chapter. For each test case, further simplification is done in Chapter 3. Based on the simplified equation system, two multiphase turbulence models are introduced in Chapter 4.

CHAPTER 3. TWO CANONICAL TEST CASES FOR PARTICLE–LADEN TURBULENT FLOWS

In this chapter, the two canonical test cases for particle-laden turbulent flows are described and the governing equation systems for turbulent kinetic energy (TKE) from Chapter 2 are simplified for the test cases.

3.1 Particle-laden Isotropic Homogeneous Turbulent Flow

In this section, the important limiting case of the particle-laden isotropic turbulent flow under zero gravity is discussed, and major results from direct numerical simulation (DNS) of Sundaram and Collins [1] are summarized. In this limiting case the second–moment of the fluctuating velocity can be studied only with effects from interphase turbulent kinetic energy (TKE) transfer and the viscous dissipation (without influence from momentum and mass conservation equations). The simplicity of this test case enables the detailed study of the unclosed terms in the governing equations for TKE in both phases.

For a steady homogeneous turbulent flow the mean pressure gradient in the fluid phase balances gravity. Hence in zero gravity the mean pressure gradient must also be zero. The mean momentum equation system results in the trivial solution of zero mean velocity in each phase, which implies a zero mean slip velocity [3]. If the flow field is initialized with zero mean velocity in both phases, the mean slip velocities will remain zero all the time.

In the DNS study of Sundaram and Collins (called decaying turbulence hereafter in the thesis), the turbulence remains isotropic, since the simulation performed in this study neglects gravity [1]. However, experimental measurements [22] and DNS calculations of Squires et al. [23, 24] report preferential concentration of particles in isotropic turbulence. While these

results indicate that particle–laden turbulent flow may not remain isotropic instantaneously on every realization, the degree to which averaged quantities like TKE in the fluid and particle phases are influenced by preferential concentration in these flows is an open question.

In the DNS [1], rigid, spherical, solid particles evolve in a free decaying isotropic turbulent flow. There is no interphase mass transfer. The flow is volumetrically dilute, with particle density much larger than fluid density ($\rho_p/\rho_f \approx 10^3$). The particle size is in the sub-Kolmogorov range ($\eta = 0.035$ and $d/\eta < 1$), but sufficiently large so that the Brownian motion of particles can be ignored. Hence, a linear drag law can be applied to each particle in the momentum equations.

The boundary layer around each particle is not calculated, and particles are viewed as point sources of momentum in the flow field [1]. The particle collisions are assumed to be elastic and conserve particle kinetic energy. As the particle volumetric loading rate is quite low, the influences of the particles on the fluid phase continuity equation are neglected, but the effects on fluid momentum are still taken into consideration.

The predictions from DNS calculation show that the energy in both phases decreases monotonically and the net effect of particles is to reduce fluid energy. This effect grows with increasing Stokes numbers. See Fig. 3.2. The particle energy also decays in time and the decay rate increases with increasing Stokes number (for fixed mass loading). See Fig. 3.3.

The simplifications to the mean equation system arise from the assumption of statistical homogeneity and zero gravity [3]. Based on the phase mean momentum equation for homogeneous, one–dimension problems, the gradient of mean pressure along the non–zero velocity component is needed to balance the acceleration due to the gravity. For the zero gravity case, the mean momentum equation for homogeneous, one dimensional flow problem shows trivial steady solutions, since the mean pressure gradient along the non-zero velocity component is zero, and also the pressure field is statistically homogeneous. If the mean velocity in each phase is initialized with zero, the mean velocity field will keep zero, which implies a zero mean slip velocity.

[1] However, kernel averaging is done to interpolate the interphase momentum through some terms onto fluid motions

With these simplifications, the evolution of energy in the fluctuating particle velocity and the TKE in the fluid phase can be studied, independent of the mean flow quantities. If zero interphase mass transfer, statistically homogeneous flow with constant thermodynamic density in both phases, and a solid dispersed phase with zero gradient of stress in the bulk are considered, the simplified governing equations are

$$\begin{aligned} \alpha_f \rho_f \frac{dk_f}{dt} &= \left\langle u_i''^{(f)} \frac{\partial (I_f \tau_{ki})}{\partial x_k} \right\rangle + \left\langle u_i''^{(f)} S_{Mi}^{(f)} \right\rangle \\ \alpha_p \rho_p \frac{dk_p}{dt} &= \left\langle u_i''^{(p)} S_{Mi}^{(p)} \right\rangle \end{aligned} \tag{3.1}$$

where α_f and α_p are the volume fraction of fluid and particle phases respectively. ρ_f and ρ_p are the density in each phases. The kinetic energy of fluctuating velocity, denoted k_f and k_p in the fluid and particle phase, is one half times the trace of the Reynolds stress tensor in the fluid and particle respectively, which is defined as

$$R_{ij}^{(\beta)} = \frac{\langle I_\beta \rho u_i''^{(\beta)} u_i''^{(\beta)} \rangle}{\langle I_\beta \rho \rangle} \tag{3.2}$$

In Eq. 3.1, $S_{Mi}^{(f)}$ and $S_{Mi}^{(p)}$ represent the interphase momentum transfer source term in each phase. The fluctuating velocity in each phase is defined in Eq. 2.18 in Chapter 2.

3.2 Particle-laden Homogeneous Shear Flow

In this section, another canonical test case, the particle-laden homogeneous shear flow, is described. Direct numerical simulations (DNS) data for this case has been reported by Elghobashi [20]. In this DNS calculation, the two-way coupling between particles and fluid is studied in a homogeneous turbulent shear flow (hereafter called homogeneous shear flows in later chapters).

In this DNS calculation, the cases with and without gravity are studied. The DNS results without gravity is compared with model results in the thesis. The sketch of the flow field is shown in Fig. 3.1. The flow field has imposed mean velocity in x_1 direction ($U = Sx_3$), where S is the mean velocity gradient, given by $S = 1$ in the simulations. The solid particles are rigid and spherical, and have constant thermodynamic density. The interphase mass transfer

is zero. The particle volume fraction is small $\alpha_p \leq 10^{-3}$, and the effect of the presence of particles on the fluid continuity equation is neglected in the DNS calculations. The particle size is in sub-Kolmogorov range. The point particle approximation is also used in this study, and the linear drag law is applied in the mean momentum equation for the fluid phase. In the DNS study, the particle–fluid density ratio (ρ_p/ρ_f) varies from 472.5 to 1890, and also the particle Stokes number (τ_p/τ_η) changes from 0.233 to 2.33.

In the fluid phase, mean velocity is imposed to x_1 direction with zero mean velocity in x_2 and x_3 directions, and the mean velocity gradient $S = dU/dx_3 = 1$, see the schematic of the flow configuration Fig. 3.1. For the particle phase, the same mean velocity field and mean velocity gradient are imposed. One can write out the governing equations for mean mass and momentum conservation in fluid and particle phase as,

$$\frac{\partial \alpha_f}{\partial t} + \langle U_1^{(f)} \rangle \frac{\partial \alpha_f}{\partial x_1} = 0, \tag{3.3}$$

$$\alpha_f \rho_f \frac{\partial \langle U_1^{(f)} \rangle}{\partial t} = -\frac{\partial \langle I_f P \rangle}{\partial x_1} + \langle S_{M1}^{(f)} \rangle, \tag{3.4}$$

$$\alpha_p \rho_p \frac{\partial \langle U_1^{(p)} \rangle}{\partial t} = -\langle S_{M1}^{(f)} \rangle. \tag{3.5}$$

In the above equation system, if the mean velocity field and the mean velocity gradient are

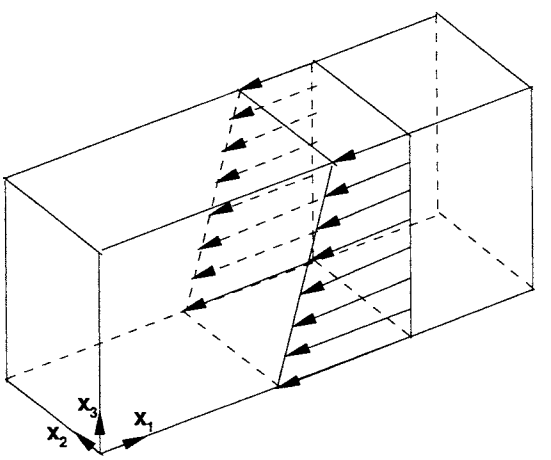

Figure 3.1 Schematic of the flow configuration in particle-laden homogeneous shear flow.

imposed (or fixed) in both fluid and particle phases, which means that the mean velocity does

not change with time in both phases. Therefore, the mean slip velocity $\langle U_1^{(f)} \rangle - \langle U_1^{(p)} \rangle$ is zero in homogeneous shear flow. Hence, the interphase momentum transfer source term $\langle S_{M1}^{(f)} \rangle$ in fluid phase should be zero, and thus the mean pressure gradient is zero everywhere.

A noteworthy point is that the flow field studied here is different from the single-phase homogeneous shear flows. In single-phase turbulence, the homogeneous shear turbulent flow can be reasonable well approximated in wind–tunnel experiments. By controlling the flow resistance upstream, a turbulent flow with the mean velocity sketched in Fig. 3.1 can be produced [25]. However, for gas–solid two–phase turbulent flow, to maintain the zero mean slip velocity and the same mean velocity gradient in both phases is quite difficult. Since the particles have much larger inertia than the fluid, particle reacts slower to the surrounding fluid. As the drag force acting on each particle depends on the slip velocity on each particles, the mean slip velocity might not remain zero as time evolves, unless there is some external force exerted on each particle. Furthermore whether the mean velocity gradient in each phase can remain same is an open question.

The major results from particle–laden homogeneous shear flows are that

i) The effect of varying the particle inertia ($\tau_p = 0.1, 0.25, 0.5, 1.0$) on the evolution of turbulent kinetic energy is studied. It shows that as the particle inertia increases, the rate of reduction of turbulence kinetic energy is increased with the largest rate of reduction observed for $\tau_p = 1.0$.

ii) The evolution of the velocity correlation $\langle u_{f,1} u_{f,3} \rangle$ is reported for $\tau_p = 1.0$ and mass loading $\phi = 1.0$. The model results for velocity correlation are compared with DNS results.

For this particle-laden homogeneous shear flow, the governing equations for the TKE in each phase can be further simplified as

$$\alpha_\beta \rho_\beta \frac{dk_\beta}{dt} = -\frac{1}{2}\frac{\partial}{\partial x_k}\alpha_\beta \rho_\beta \langle u_i''^{(\beta)} u_i''^{(\beta)} u_k''^{(\beta)} \rangle - \left\{ \alpha_\beta \rho_\beta \langle u_1''^{(\beta)} u_3''^{(\beta)} \rangle \frac{\partial \langle \tilde{U}_1^{(\beta)} \rangle}{\partial x_3} \right\} + \langle u_i''^{(\beta)} \frac{\partial (I_\beta \tau_{ki})}{\partial x_k} \rangle + \langle u_i''^{(\beta)} S_{Mi}^{(\beta)} \rangle \tag{3.6}$$

where in shear production term, only $dU_1/dx_3 \neq 0$. The Reynolds stress $R_{13}^{(\beta)} = \langle u_1''^{(\beta)} u_3''^{(\beta)} \rangle$ remains after the simplification. All the other terms have been discussed in Chapter 2. In the

multiphase turbulence models tested in this work, the triple correlation of fluctuating velocity is usually modeled with a gradient-diffusion hypothesis

$$\frac{\partial}{\partial x_k}\alpha_\beta\rho_\beta\langle u_i''^{(\beta)}u_i''^{(\beta)}u_k''^{(\beta)}\rangle = -\frac{\partial}{\partial x_k}\left(\alpha_\beta\rho_\beta\frac{\nu_T}{\sigma_k}\frac{\partial k_\beta}{\partial x_3}\right)$$

where ν_T is the turbulent eddy viscosity in each phase, and σ_k is the turbulent Prandtl number for kinetic energy, which is generally taken to be 1.0. Since the turbulent flow field is homogeneous, the triple correlation is omitted in the equation system. The evolution equation for TKE for phase β is further simplified as

$$\alpha_\beta\rho_\beta\frac{\partial k_\beta}{\partial t} = -\left\{\alpha_\beta\rho_\beta\langle u_1''^{(\beta)}u_3''^{(\beta)}\rangle\frac{\partial\langle\tilde{U}_1^{(\beta)}\rangle}{\partial x_3}\right\} + \langle u_i''^{(\beta)}\frac{\partial(I_\beta\tau_{ki})}{\partial x_k}\rangle + \langle u_i''^{(\beta)}S_{Mi}^{(\beta)}\rangle \qquad (3.7)$$

In Chapter 4, two multiphase turbulence models are simplified following the formulation in Eq. 3.7. Some deficiencies with these two multiphase turbulence models are found out.

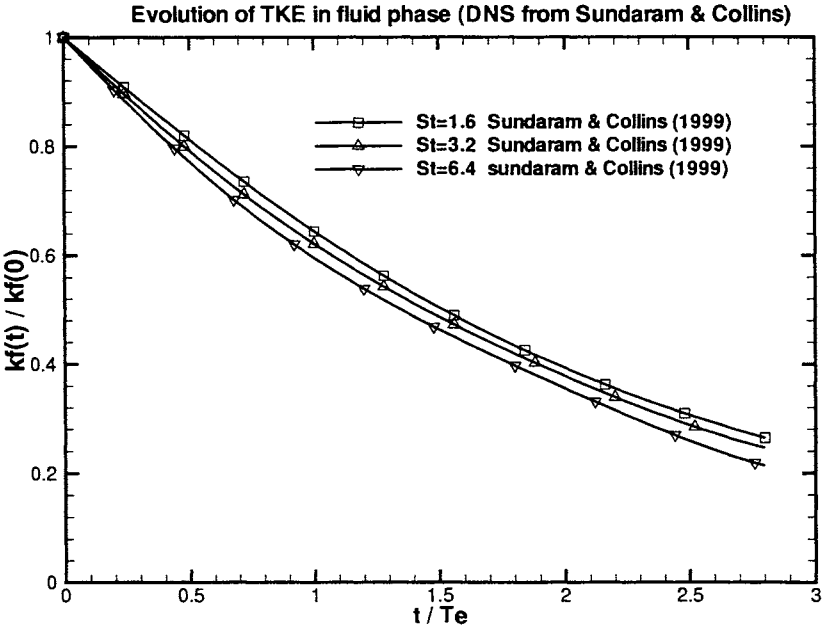

Figure 3.2 Evolution of normalized TKE in fluid phase (DNS data from Sundaram and Collins [1]).

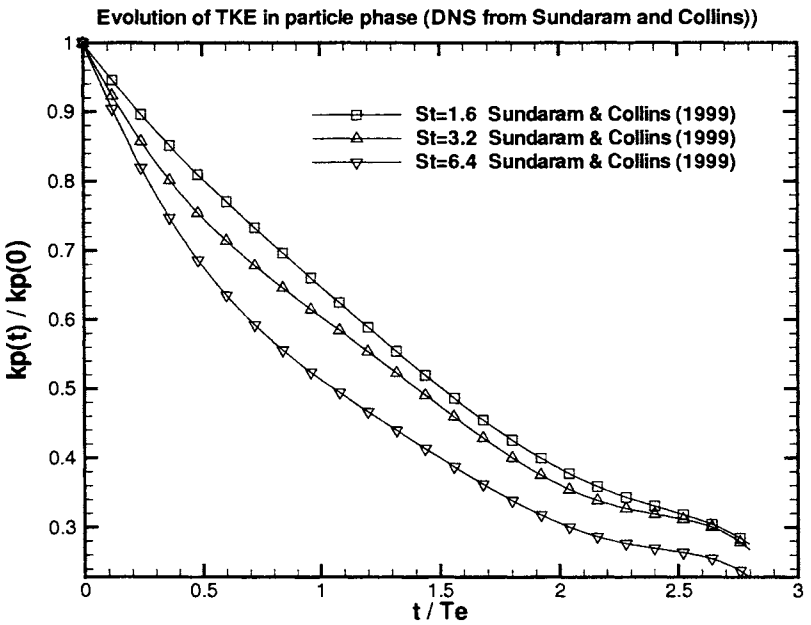

Figure 3.3 Evolution of particle energy (DNS data from Sundaram and Collins [1]).

CHAPTER 4. DESCRIPTION OF MULTIPHASE TURBULENCE MODELS

Two multiphase turbulence models that are tested are described in this chapter. The governing equations from these two models are further simplified for decaying isotropic turbulence (particle-laden isotropic turbulent flows) and the particle-laden homogeneous shear flows. In order to do the comparative assessmemt, the simplified model equations are solved numerically. Some numerical stiffness problem is found when solving the model equations. This stiffness problem is analyzed and discussed in Section 3, and also the numerical method used is described in this section.

4.1 Simonin's Model: Model Description

The model proposed by Simonin and co-workers uses the Eulerian–Eulerian approach for both phases in the gas–solid turbulent flows. The turbulent motion in fluid phase is predicted by means of a standard two–equation single phase turbulence model (the widely employed $k-\varepsilon$ model), with additional terms for interactions with the dispersed phase.

For the dispersed phase, a separate transport equation for the particulate kinetic stress tensor is derived, which accounts for the turbulent transport mechanism, and the drag force. The trace of particle kinetic stress tensor is actually the TKE in particle phase. The model for particle phase TKE is restricted to relatively low particle concentrations (particle volume fraction $\alpha_p < 0.1$, and the inter–particle collisions are neglected). The turbulent momentum transfer between two phases is represented through a fluid–particle velocity covariance (k_{fp}), which obeys an additional transport equation.

4.1.1 Governing Equations for Particle–laden Isotropic Turbulence

The simplified model equations for TKE k_f and dissipation rate ε_f in fluid phase [1] are

$$\begin{aligned} \alpha_f \rho_f \frac{dk_f}{dt} &= \Pi_{k_f} - \alpha_f \rho_f \varepsilon_f, \qquad (4.1) \\ \alpha_f \rho_f \frac{d\varepsilon_f}{dt} &= \Pi_{\varepsilon_f} - \alpha_f \rho_f \frac{\varepsilon_f^2}{k_f} C_{\varepsilon_2}. \qquad (4.2) \end{aligned}$$

where $C_{\varepsilon_2} = 1.92$. Particle phase influences the fluid phase TKE through the interphase TKE transfer term Π_{k_f}, which is modeled as,

$$\Pi_{k_f} = \alpha_p \rho_f F_D \left[k_{fp} - 2k_f + (U_{f,i} - U_{p,i}) \cdot U_{d,i}\right]. \qquad (4.3)$$

where F_D defined below, plays the role of an effective particle response frequency. Due to the zero mean slip in the flow, Π_{k_f} is further simplified as,

$$\Pi_{k_f} = \alpha_p \rho_f F_D \left[k_{fp} - 2k_f\right] \qquad (4.4)$$

The particle influence on the dissipation rate of fluid energy ε_f in Eq. 4.2 is,

$$\Pi_{\varepsilon_f} = C_{\varepsilon,3} \frac{\varepsilon_f}{k_f} \Pi_{k_f}. \qquad (4.5)$$

where $C_{\varepsilon,3} = 1.2$.

The modeled transport equation for TKE in particle phase is simplified as

$$\begin{aligned} \alpha_p \rho_p \frac{dk_p}{dt} &= \Pi_{k_p}, \\ \alpha_p \rho_p \frac{dk_{fp}}{dt} &= \Pi_{k_{fp}} - \alpha_p \rho_p \varepsilon_{fp}. \qquad (4.6) \end{aligned}$$

The dissipation of the particle energy is neglected, due to the assumption of elastic collisions in the DNS studies.

The interaction term accounting for the influence of fluid phase on k_p is modeled as

$$\Pi_{k_p} = -\alpha_p \rho_p \frac{1}{\tau_{12}^F} \left[2k_p - k_{fp}\right] \qquad (4.7)$$

[1] In Simonin's model, 1 represents the fluid or carrier phase; 2 represents the particle or dispersed phase. Here subscript f is used to represent the fluid phase; and subscript p to represent the particle phase.

where τ_{12}^F is the particle relaxation time [2] In the dynamic equation of fluid–particle covariance k_{fp}, the interphase momentum transfer is given by

$$\Pi_{k_{fp}} = -\alpha_p \rho_p \frac{1}{\tau_{12}^F} \left[(1+\phi)\, k_{fp} - 2k_f - 2\phi k_p \right], \tag{4.8}$$

where $\phi = \frac{\alpha_p \rho_p}{\alpha_f \rho_f}$ is the mass loading. The term ε_{fp} accounts for the dissipation rate due to viscosity in the fluid phase and the loss of correlation by crossing-trajectory effects, which is modeled as

$$\varepsilon_{fp} = k_{fp}/\tau_{12}^t \tag{4.9}$$

where τ_{12}^t is the time scale of the fluid turbulent motion viewed by the particles, and is modeled as

$$\tau_{12}^t = \tau_1^t \left[1 + c_\beta \xi_r^2 \right]^{-1/2} \quad \text{where} \quad \xi_r = \frac{|\bar{V}_r|}{\sqrt{\frac{2}{3} k_f}}$$

where c_β varies with the angle between the mean particle velocity and the mean relative velocity, and $c_\beta = 0.45$, since this angle is zero in homogeneous turbulence case. The time scale of the energetic turbulent eddies τ_1^t is

$$\tau_1^t = \frac{3}{2} C_\mu \frac{k_f}{\varepsilon_f}$$

where $C_\mu = 0.09$.

The effective particle response frequency F_D is given in terms of local mean particle Reynolds number Re_p:

$$\begin{aligned} F_D &= \frac{3}{4} \frac{C_D}{\bar{d}} \langle |\overline{v}_r| \rangle, \quad \langle |\overline{v}_r| \rangle = \sqrt{V_{r,i} V_{r,i} + \langle v''_{r,i} v''_{r,i} \rangle_2} \\ C_D &= \frac{24}{Re_p} \left[1 + 0.15 {Re_p}^{0.687} \right] \alpha_f^{-1.7}, \quad \text{for} \quad Re_p < 1000 \end{aligned}$$

where the particle Reynolds number Re_p is defined as,

$$Re_p = \frac{\alpha_f \langle |\overline{v}_r| \rangle \bar{d}}{\nu_f}. \tag{4.10}$$

The averaging method $\langle \cdot \rangle_2$ is defined as the dispersed phase mass average in Simonin's model. The average value of the local relative velocity between each particle and the surrounding fluid

[2] In chapter 6, the notation for particle relaxation time changes to τ_p.

flow $V_{r,i}$ can be expressed as

$$V_{r,i} = [U_{p,i} - U_{f,i}] - V_{d,i} \qquad V_{d,i} = \langle \tilde{u}_{f,i} \rangle_2 - U_{f,i} = \langle u''_{f,i} \rangle_2 \tag{4.11}$$

where $U_{p,i}$ and $U_{f,i}$ are the mean velocity of each phase; the drifting velocity $V_{d,i}$ represents the correlation between the instantaneous distribution of particles and the turbulent fluid motion at large characteristic length scale with respect to the particle diameter.

The principal time scale in the model is τ_{12}^F, the particle relaxation time or response time, which is related to the inertial effects acting on the particles:

$$\tau_{12}^F = F_D^{-1} \frac{\rho_p}{\rho_f} \tag{4.12}$$

However, this time scale is based on the slip velocity $\langle |\bar{v}_r| \rangle_2$, which is defined on the basis of $u'_f \sim \sqrt{k_f}$ and $u'_p \sim \sqrt{k_p}$.

The model constants used in Simonin's model are listed in Table 4.1.

Table 4.1 List of coefficients for Simonin's model

C_μ	$C_{\varepsilon,2}$	$C_{\varepsilon,1}$	σ_q	σ_ε	σ_1	$C_{\varepsilon,3}$
0.09	1.92	1.44	1.0	1.3	1.0	1.2

4.1.2 Governing Equations for Particle–laden Homogeneous Shear Flow

For the particle-laden homogeneous shear flow discussed in Chapter 3, the mean velocity is only non-zero in x_1 direction, and $S = dU_1/dx_3 = 1$; see Fig. 3.1.

The simplified model equations for TKE k_f and dissipation rate ε_f in fluid phase are

$$\frac{dk_f}{dt} = -\langle u''_{f,1} u''_{f,3} \rangle \frac{\partial U_{f,1}}{\partial x_3} + \frac{\Pi_{k_f}}{\alpha_f \rho_f} - \varepsilon_f \tag{4.13}$$

$$\frac{d\varepsilon_f}{dt} = -\frac{\varepsilon_f}{k_f} C_{\varepsilon,1} \langle u''_{f,1} u''_{f,3} \rangle \frac{\partial U_{f,1}}{\partial x_3} + \frac{\Pi_{\varepsilon_f}}{\alpha_f \rho_f} - C_{\varepsilon,2} \frac{\varepsilon_f^2}{k_f} \tag{4.14}$$

The interphase TKE transfer term and dissipation term have been discussed in the previous section. The production of TKE in both phases due to the mean velocity gradient takes effect in this case. The fluid velocity correlation is computed with the help of turbulent eddy viscosity

concept in Simonin's model,

$$\langle u''_{f,i} u''_{f,j} \rangle = -\nu_f^t \left[\frac{\partial U_{f,i}}{\partial x_j} + \frac{\partial U_{f,j}}{\partial x_i} \right] + \frac{2}{3} \delta_{ij} \left[k_f + \nu_f^t \frac{\partial U_{f,m}}{\partial x_m} \right] \tag{4.15}$$

where the turbulent eddy viscosity in fluid phase is modeled as

$$\nu_f^t = \frac{2}{3} k_f \tau_1^t = C_\mu \frac{k_f^2}{\varepsilon_f} \tag{4.16}$$

where $C_\mu = 0.09$.

The simplified equations for TKE in particle phase are

$$\frac{dk_p}{dt} = -\langle u''_{p,1} u''_{p,3} \rangle \frac{\partial U_{p,1}}{\partial x_3} + \frac{\Pi_{k_p}}{\alpha_p \rho_p} \tag{4.17}$$

$$\frac{dk_{fp}}{dt} = -\langle u''_{f,1} u''_{p,3} \rangle \frac{\partial U_{p,1}}{\partial x_3} - \langle u''_{f,3} u''_{p,1} \rangle \frac{\partial U_{f,1}}{\partial x_3} + \frac{\Pi_{k_{fp}}}{\alpha_p \rho_p} - \varepsilon_{fp} \tag{4.18}$$

The turbulent kinetic stress tensor components are modeled using the turbulent eddy–viscosity concept:

$$\langle u''_{p,i} u''_{p,j} \rangle = -\nu_p^t \left[\frac{\partial U_{p,i}}{\partial x_j} + \frac{\partial U_{p,j}}{\partial x_i} \right] + \frac{2}{3} \delta_{ij} \left[k_p + \nu_p^t \frac{\partial U_{p,m}}{\partial x_m} \right] \tag{4.19}$$

The algebraic expression for the turbulent eddy–viscosity in particle phase is obtained from the off–diagonal correlation equations written in a quasi–equilibrium homogeneous shear flow, assuming that the difference between the fluid and the particle mean velocity gradients remains negligible:

$$\nu_p^t = \left[\nu_{12}^t + \frac{1}{2} \tau_{12}^F \frac{2}{3} k_p \right] \left[1 + \frac{\tau_{12}^F}{2} \frac{\sigma_c}{\tau_2^c} \right]^{-1} \tag{4.20}$$

where τ_2^c is the inter-particle collision time and σ_c takes the general form,

$$\sigma_c = [1 + e_c][3 - e_c]/5 \tag{4.21}$$

Since the inter-particle collision is assumed to be elastic ($e_c = 1$) in the DNS case, σ_c leads to the Grad's value $\sigma_c = 0.45$. Following Simonin's discussion [26], if τ_2^c is small compared to the other time scales, the particle fluctuating motion is controlled by collisions between particles without effects from the fluid motion. On the other hand, if τ_2^c is large, the gas is expected to play a dominant role in the fluid fluctuating motion of particles. So for very dilute gas-solid

two-phase flows, τ_2^c is expected to be very large ($\tau_2^c \to \infty$). The turbulent eddy-viscosity in particle phase for the dilute particle-laden flows is further simplified as

$$\nu_p^t = \nu_{fp}^t + \frac{1}{2}\tau_{12}^F \frac{2}{3} k_p \tag{4.22}$$

The fluid-particle turbulent viscosity ν_{fp}^t is written in terms of the fluid-particle velocity covariance k_{fp} and an eddy-particle interaction time τ_{12}^t,

$$\nu_{fp}^t = \frac{1}{3} k_{fp} \tau_{12}^t \tag{4.23}$$

The fluid–particle covariance must be modeled, and there is no direct measurement of the quantity. The closure assumption for this term is made to be consistent with the modeling of fluid turbulence when the particle response time tends toward zero with respect to the eddy–particle interaction time

$$\begin{aligned} \langle u''_{f,i} u''_{p,j} \rangle = & \frac{1}{3} k_{fp} \delta_{ij} + \frac{\eta_f}{1+\eta_r} \left[\langle u''_{f,i} u''_{f,j} \rangle - \frac{2}{3} k_f \delta_{ij} \right] \\ & - \frac{\nu_{12}^t}{1+\eta_r} \left[\frac{\partial U_{f,i}}{\partial x_j} + \frac{\partial U_{p,j}}{\partial x_i} - \frac{1}{3} \frac{\partial U_{f,m}}{\partial x_m} \delta_{ij} - \frac{\partial U_{p,m}}{\partial x_m} \delta_{ij} \right] \end{aligned} \tag{4.24}$$

where $\eta_r = \tau_{12}^t / \tau_{12}^F$. If τ_{12}^F is very small compared with τ_{12}^t, the fluid-particle covariance is given by

$$\langle u''_{f,i} u''_{p,j} \rangle = \frac{1}{3} k_{fp} \delta_{ij} + \langle u''_{f,i} u''_{f,j} \rangle - \frac{2}{3} k_f \delta_{ij} \tag{4.25}$$

4.1.3 Initialization of Certain Model Parameters

In Simonin's model, the auxiliary flow quantities need to be initialized. One of these unspecified quantities is $\langle |v_r| \rangle_2$, the magnitude of the averaged value of the local relative velocity between each particle and the surrounding fluid flows. In Simonin's model $\langle |v_r| \rangle_2$ is defined as

$$\langle |v_r| \rangle_2 = \sqrt{V_{r,i} V_{r,i} + \langle v''_{r,i} v''_{r,i} \rangle_2}$$

where $V_{r,i}$ is the mean relative or slip velocity, and is zero in the particle–laden isotropic turbulent flows. In $\langle |v_r| \rangle_2 \; v''_{r,i}$ needs to be modeled. In the thesis, the following approximations are used

$$v''_{r,i} \equiv \alpha_f \alpha_p \left(u'_f + u'_p \right) \quad \text{where} \quad u'_f = \sqrt{\frac{2}{3} k_f} \;\; , \;\; u'_p = \sqrt{\frac{2}{3} k_p}. \tag{4.26}$$

In addition, in Simonin's model, the fluid-particle velocity covariance k_{fp} is a pseudo–flow quantity, and needs to be initialized[3]. An approximation is used here for k_{fp}

$$k_{fp}(t) = \rho_{fp}(t) \cdot k_f^{1/2}(t) \cdot k_p^{1/2}(t) \tag{4.27}$$

where $\rho_{fp}(t)$ is a "fluid-particle" correlation coefficient, which should be bounded between 0 and 1, based on Cauchy–Schwarz inequality.[4] Using this definition, we can determine $k_{fp}(0)$ by setting $\rho_{fp}(0)$ values. The role of k_{fp} is discussed in detail by Subramaniam who argued that k_{fp} has no place in first-order single point closures of two-phase turbulent flows. This conclusion is also reached in the DNS study of Collins in Eq. (29c,d) in [1].

4.2 Ahmadi's Model: Model Description

A two–equation model is derived for TKE in fluid and particle phases by Ahmadi [7]. The dissipation rate of fluid and particle energy is given by a set of algebraic equations. Model predictions of simple shear flows for a dense mixture are reported [8] and the particle volume fraction employed in this validation is up to 0.3 for gas-solid turbulent shear flows. The governing equations for the transport of mass, momentum, and fluctuation energy are derived specially for the case of an isothermal, fully saturated two–phase flow with incompressible fluid and particulate constituents [8].

4.2.1 Governing Equations for Particle-laden Isotropic Turbulence

The simplified TKE governing equations for the the particle–laden isotropic turbulent flows are [5]

$$\rho_f \alpha_f \frac{dk_f}{dt} = 2D_0 \left(k_p - ck_f\right) - \rho_f \alpha_f \varepsilon_f \tag{4.28}$$

$$\rho_p \alpha_p \frac{dk_p}{dt} = 2D_0 \left(ck_f - k_p\right) \tag{4.29}$$

[3] In general, for inhomogeneous flows, one needs to specify this pseudo–flow quantity for boundary conditions, which makes the problem even more complicated.

[4] Some researchers [14] define ρ_{fp} up to 2. In this work, $\rho_{fp}(0) = 2.0$ is used.

[5] In Ahmadi's model, the notation to represent the fluid and particle phase, and volume fraction are slightly different. The notations are made consistent in the thesis.

The dissipation rate for energy in the fluid phases is modeled as

$$\varepsilon_f = a_f \left(k_f\right)^{3/2} \quad \text{and} \quad a_f = \frac{C_{fD}}{\Lambda_f} \tag{4.30}$$

where $C_{fD} = 0.165$ is a constant and Λ_f is a characteristic length of fluid turbulence. Since particle collisions are elastic in the DNS test case, the dissipation rate of particle energy is taken to be zero in Ahmadi's model.

The coefficient c is related to the ratio of the particle time scale $\rho_p \alpha_p / D_0$ to the Lagrangian time macroscale of turbulence T_L,

$$c = \frac{1}{1 + \frac{\rho_p \alpha_p}{D_0 T_L}}, \quad T_L = \frac{0.165 k_f}{\varepsilon_f}.$$

The drag coefficient is given as

$$D_0 = \frac{18 \mu_f \alpha_p}{\bar{d}^2} \frac{\left[1 + 0.1 \left(Re_p\right)^{0.75}\right]}{\left(1 - \frac{\alpha_p}{\nu_m}\right)^{0.25 \nu_m}}$$

where $\bar{d}$ is the mean particle diameter. The particle Reynolds number Re_p is defined as

$$Re_p = \frac{\rho_f \bar{d} |U_{f,i} - U_{p,i}|}{\mu_f}.$$

where $U_{f,i}$ and $U_{p,i}$ are the i^{th} component of the mean velocity in the fluid and particle phase respectively.

4.2.2 Governing Equations for Particle–laden Homogeneous Shear Flow

The simplified governing equations for TKE evolution in each phase for particle–laden homogeneous shear flows are,

$$\rho_f \alpha_f \frac{dk_f}{dt} = \mu_f^t \frac{\partial U_{f,1}}{\partial x_3} \frac{\partial U_{f,1}}{\partial x_3} + 2 D_0 \left(k_p - c k_f\right) - \rho_f \alpha_f \varepsilon_f \tag{4.31}$$

$$\rho_p \alpha_p \frac{dk_p}{dt} = \mu_p^t \frac{\partial U_{p,1}}{\partial x_3} \frac{\partial U_{p,1}}{\partial x_3} + 2 D_0 \left(c k_f - k_p\right) \tag{4.32}$$

The dissipation term and the interphase TKE transfer term in Ahmadi's model are discussed in the previous section. The fluid phase Reynolds stress tensor is modeled using the turbulent eddy–viscosity concept,

$$\tau_{ij}^{(f)} = -\langle \rho_f u''_{f,i} u''_{f,j} \rangle = -\frac{2}{3} \left(\alpha_f \rho_f k_f + \mu_f^t \frac{\partial U_{f,m}}{\partial x_m}\right) \delta_{ij} + \mu_f^t \left(\frac{\partial U_{f,i}}{\partial x_j} + \frac{\partial U_{f,j}}{\partial x_i}\right) \tag{4.33}$$

where the turbulent eddy–viscosity in the fluid phase is modeled identically to that in the single–phase turbulence,

$$\mu_f^t = \frac{C_\mu \alpha_f \rho_f k_f^2}{\varepsilon_f} \tag{4.34}$$

The velocity correlation in the particle phase is similarly modeled as,

$$\tau_{ij}^{(p)} = -\langle \rho_p u''_{p,i} u''_{p,j} \rangle = -\left(\gamma \alpha_p \rho_p k_p + \frac{2}{3} \mu_p^t \frac{\partial U_{p,m}}{\partial x_m} \right) \delta_{ij} + \mu_p^t \left(\frac{\partial U_{p,i}}{\partial x_j} + \frac{\partial U_{p,j}}{\partial x_i} \right) \tag{4.35}$$

where γ is a function of the particle volume fraction α_p. The turbulent eddy viscosity μ_p^t is modeled as

$$\mu_p^t = C_\mu^p \rho_p \alpha_p d \sqrt{k_p} \tag{4.36}$$

where C_μ^p is

$$C_\mu^p = 0.0853[(\chi \alpha_p)^{-1} + 3.2 + 12.1824 \alpha_p \chi] \tag{4.37}$$

and χ is the particle radial distribution function, which describes the crowding effect of the particles,

$$\chi = \frac{1 + 2.5\alpha_p + 4.5904\alpha_p^2 + 4.515439\alpha_p^3}{\left[1 - \left(\frac{\alpha_p}{\nu_m}\right)^3\right]^{0.678021}} \tag{4.38}$$

with $\nu_m = 0.64356$. The increase in the particulate pressure is accounted for through the coefficient γ which is given as

$$\gamma = \frac{2}{3}(1 + 4\alpha_p \chi) + \frac{1}{3}(1 - r^2) \tag{4.39}$$

with the restitution coefficient $r = 1$ in the DNS case.

The viscosity in particle phase is a function of the solid volume fraction α_p, TKE in particle phase k_p and some length scale. This length scale is chosen as the mean particle diameter $\bar{d}$ in Ahmadi's model, which is especially designed for the relative dense collision–dominated mixture flows[7]. For dilute mixtures, the fluid turbulence dominates and the particles are essentially transported by the fluid phase. Thus it is suggested by Besnard and Harlow in [27] that the length scale in the fluid phase is the appropriate length scale in this situation.

4.2.3 Initialization of Certain Model Parameters

The model constants used in Ahmadi's model are listed in Table 4.2. In Ahmadi's model, Λ_f is a length of fluid turbulence, which is required to match the initial fluid dissipation rate in DNS test case and a relation is required to connect Λ_f with ε_f as time evolves. For the isotropic homogeneous turbulent flow, the fluid phase turbulent motion can be approximated by the grid turbulence.

Table 4.2 List of coefficients for Ahmadi's model

C_{fD}	ν_m	C_μ
0.65	0.64356	0.09

From grid turbulence experiments, the power law decay of TKE is given as,

$$k(t) = k_0 \left(\frac{t}{t_0}\right)^{-n}$$

and

$$\varepsilon(t) = \varepsilon_0 \left(\frac{t}{t_0}\right)^{-(n+1)}$$

where t_0 is the arbitrary reference time, k_0 is the value of k at that time. The value of decay exponent n can be chosen between 1.15 and 1.45; Mohamed and LaRue [28] suggest that nearly all of the data are consistent with $n = 1.3$ [25].

In Ahmadi's model, a_f can be approximated as

$$a_f = \frac{k^{3/2}}{\varepsilon} \sim \left(\frac{t}{t_0}\right)^{(1-n/2)} = \left(\frac{t}{t_0}\right)^{0.35} \tag{4.40}$$

and Λ_f can be determined from the above relations as time evolves. The arbitrary reference time scale is determined by the initial k_f and ε_f in DNS test case.

For the particle-laden homogeneous shear flows, the fluid phase turbulent motion cannot be approximated by such physical model. Since the length scale used in μ_f^t is not a closed term in this model, Ahmadi's model is not tested in the homogeneous shear flows in the thesis.

4.3 Numerical Stiffness Problem in Solving the Model Equations

The multiphase turbulence models discussed in this chapter, are all simplified to a set of ordinary differential equations for the test cases, since the test cases are homogeneous in space and all the spatial derivatives can be neglected. It is found that for particle–laden isotropic turbulent flows, if increasing the particle volume fraction to 10^{-3} and keeping the density ratio fixed, the equation system from both models cannot be solved using the simple Euler scheme if the step length is scaled as a fraction of particle response time τ_{12}^F, which is a constant in both test cases. With more accurate numerical methods, such as Runge–Kutta 4^{th} order method, the solutions are not stable if the step length is scaled in the same way as it is mentioned before. In general, if the equation systems from both models are solved with particle volume fraction increased and density ratio kept the same, the results are not stable for simple Euler scheme and Runge–Kutta 4^{th} order method if the step length is a fraction of a constant, the particle response time in the models. The phenomenon exhibited here is known as *stiffness*. Both equation systems from the simplified multiphase turbulence models are *stiff systems*.

To understand the concept of stiffness better, the mathematical statement used to describe the notion of stiffness is introduced in this section and equation system from Ahmadi's model is studied in detail[29].

Some mathematical definitions are introduced first. The first-order system $\dot{y} = f(t, y)$ is said to be *linear* if $f(t, y)$ takes the form $f(t, y) = A(t)y + \psi(t)$. Furthermore, if A is independent of t, the system is said to be *linear with constant coefficients*. Associated with such a system

$$\dot{y} = Ay + \psi(t) \tag{4.41}$$

is the homogeneous form

$$\dot{y} = Ay \tag{4.42}$$

where y and ψ are vectors in real space $\mathbb{R}^m$ and A is a $m \times m$ real matrix with eigenvalues $\lambda_i \in \mathbb{C},\ i = 1, 2, \ldots, m$ and the corresponding eigenvector $c_i \in \mathbb{C}^m,\ i = 1, 2, \ldots, m$. The

general solution of Eq. 4.42 is

$$y(t) = \sum_{i=1}^{m} \kappa_i \exp(\lambda_i t) c_i, \tag{4.43}$$

The general solution of Eq. 4.41 can be written as

$$y(t) = \sum_{i=1}^{m} \kappa_i \exp(\lambda_i t) c_i + \Psi(t), \tag{4.44}$$

where κ_i are arbitrary constants and $\Psi(t)$ is a particular integral.

Suppose the real parts of all the eigenvalues are less than zero; this implies that each of the terms $\exp(\lambda_i t)c_i \to 0$ as $t \to \infty$, so that the solution $y(t)$ approaches $\Psi(t)$ asymptotically as $t \to \infty$. The term $\exp(\lambda_i t)c_i$ will decay monotonically if λ_i is real and sinusoidally if λ_i is complex. Usually t can be interpreted as time, and it is appropriate to call $\sum_{i=1}^{m} \kappa_i \exp(\lambda_i t)c_i$ the *transient solution* and $\Psi(t)$ the *steady-state solution.* The real part of eigenvalue is denoted as $\mathrm{Re}(\lambda_i)$. If $|\mathrm{Re}(\lambda_i)|$ is large then the corresponding term $\kappa_i \exp(\lambda_i t)c_i$ decays quickly as t increases and is the fast transient; if $|\mathrm{Re}(\lambda_i)|$ is small, the corresponding term $\kappa_i \exp(\lambda_i t)c_i$ decays slowly and is a slow transient. If

$$|\mathrm{Re}(\lambda_{min})| \leq |\mathrm{Re}(\lambda_i)| \leq |\mathrm{Re}(\lambda_{max})|, \quad i = 1, 2, \ldots, m.$$

then $\kappa_i \exp(\lambda_{max} t)c_i$ is the fastest transient and $\kappa_i \exp(\lambda_{min} t)c_i$ is the slowest. If the numerical method has a finite region of absolute stability, the step length h must be sufficiently small for $|h\lambda_i|$ in the absolute stability region. Then it is clear that a large value of $|\mathrm{Re}(\lambda_{max})|$ implies a small step length. One might step into a difficult situation if the ratio between $|Re(\lambda_{max})|$ and $|Re(\lambda_{min})|$ is very large; it is required to integrate for a very long time with an excessively small step length. This ratio is usually called the stiffness ratio and can be used to measure the stiffness of a system.

Based on the analysis from a mathematical point of view, one can start with the simplified equation system for particle–laden isotropic turbulent flows from Ahmadi's model, since Ahmadi's model just has two governing equations in the system and is easier to analyze. The equation system is rewritten as

$$\frac{d}{dt}\begin{bmatrix} k_f \\ k_p \end{bmatrix} = \frac{2}{\tau_p}\begin{bmatrix} -c\phi & \phi \\ c & -1 \end{bmatrix} \cdot \begin{bmatrix} k_f \\ k_p \end{bmatrix} + \begin{bmatrix} -\varepsilon_f \\ 0 \end{bmatrix} \tag{4.45}$$

where τ_p is the particle response time and ϕ is the mass loading. It is clear that in this inhomogeneous system, the 2×2 matrix A is of rank 1 and it has the eigenvalues $\lambda_1 = 0$ and $\lambda_2 = -(c\phi + 1)$. Thus the stiffness ratio is ∞ in this situation, which means that this system is a singular system. Furthermore as mass loading increases, $|\lambda_2|$ increases linearly. The model coefficient c is actually a function of particle response time τ_p and eddy turnover time τ, and c will change with time.

To solve the homogeneous system first,

$$\frac{d}{dt}\begin{bmatrix} k_f \\ k_p \end{bmatrix} = \frac{2}{\tau_p}\begin{bmatrix} -c\phi & \phi \\ c & -1 \end{bmatrix} \cdot \begin{bmatrix} k_f \\ k_p \end{bmatrix} \tag{4.46}$$

the analytical solution of this ODE system is

$$k_f(t) = \left(\frac{\rho_m k_m}{\alpha_f \rho_f}\right)\frac{1}{1+c\beta} + \left(k_f(0) - \left(\frac{\rho_m k_m}{\alpha_f \rho_f}\right)\frac{1}{1+c\phi}\right) \cdot e^{\frac{1}{\tau_p}\cdot(1+c\phi)t} \tag{4.47}$$

where $\rho_m k_m = \rho_f k_f + \rho_p k_p$ is the total TKE per unit volume. In the analytical solution, as mass loading ϕ increases, the required step length should decrease and should be scaled as a fraction of $\frac{\tau_p}{1+c\phi}$. To solve this equation system, the simplest way is to scale the step length as a fraction of $\frac{\tau_p}{1+c\phi}$ instead of τ_p with simple Euler time stepping. The temporal convergence for the equation system from Ahmadi's model for the particle–laden isotropic turbulence shows in Fig. 4.1. The equation system is solved by some very fine time step Δt_f. Using the solution at this time step as reference, the solution solved at the coarse time step Δt_c is compared with the reference and RMS error is computed. The x axis represents the ratio $\Delta t_c / \Delta t_f$ and y axis represents the RMS error. Both axes are of log scale, and the slope of the error growing is 1.0.

For Simonin's model, the simplified equation system for particle–laden isotropic turbulent flows is a more complicate ODE system with four equations. Therefore it is quite difficult to get the eigenvalues in a symbolic form and understand the relation between $|\mathrm{Re}(\lambda_{max})|$ and mass loading ϕ. If the equation system in Simonin's model is rewritten in the homogeneous

form,

$$\dot{y} = Ay,$$

where A is a 4×4 matrix and is a function of t. By fixing all the other variables in the model and increasing the particle volume fraction α_p, the relation between the largest eigenvalues and the mass loading can be obtained numerically. It is found that the largest eigenvalue of the system at $t = 0$ grows linearly with the mass loading ϕ. However the matrix A is also a function of time t, thus the eigenvalues of this system change with time. It is found out that the growth of eigenvalues with time is small if compared with the growth of eigenvalues with increasing mass loading. The model equation can be solved stably and with a certain order of accuracy. This will be helpful when comparing numerical results from turbulence models with the DNS data.

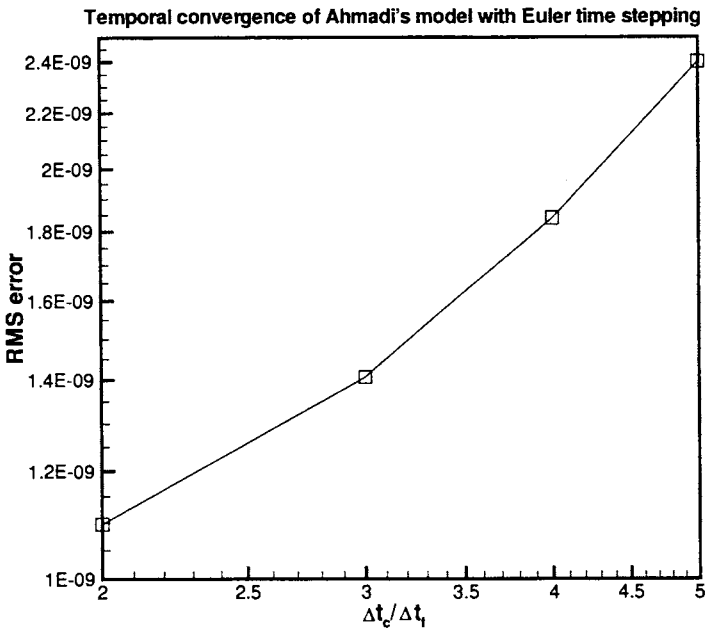

Figure 4.1 The temporal convergence of equation system from Ahmadi's model solved with Euler time stepping.

The numerical results from the model equations will be compared with DNS results for the two canonical test cases for dilute particle–laden turbulent flows in Chapter 5.

CHAPTER 5. COMPARATIVE ASSESSMENT OF MULTIPHASE TURBULENCE MODELS

In this Chapter, the predictions from Simonin and Ahmadi's models are described. The model results are compared with DNS data for the two canonical test problems. The performance of the turbulence models from Simonin and Ahmadi is verified, and some discrepancies are found. The reasons behind these anomalous model behaviors are discussed. As discussed in Chapter 4, both models need specification of some initial conditions. For Ahmadi's model, the length scale of fluid phase turbulence Λ_f is not defined in the model. For simple flow field like isotropic homogeneous turbulence, this length scale can be approximated by experiments results. For more complicated flow field, such as homogeneous shear flows, there is no such simple approximation. The following table 5.1 summarizes the cases in comparative assessment.

Table 5.1 Cases tested in the comparative assessment

	decaying homogeneous turbulence	homogeneous shear flows
Simonin's model	YES	YES
Ahmadi's model	YES	NO

From this table, it is clear that Simonin's model will be tested for both test cases, while Ahmadi's model is tested only for the decaying homogeneous particle–laden flow.

5.1 Predictions of Simonin's Model

In this section, model predictions from Simonin's model are discussed for both the decaying homogeneous turbulent flows and the homogeneous shear flows.

Decaying Homogeneous Turbulent Flow

A noteworthy point when comparing model results to DNS results for particle–laden isotropic turbulence, is the specification of appropriate initial conditions. In the DNS study, the particle velocity is initially set equal to the surrounding fluid velocity. This initial condition has a first order effect on the evolution of the dissipation rate at the early time, where the dissipation rate in fluid energy increases first then decrease (see Figure 4.(a) and (b)) in [1] for details). At longer time $t/T_e > 0.8$, one can expect that the DNS has lost the memory of the initial conditions and the results correspond to freely decaying particle-laden turbulent flows. The initial conditions used comparative assessment are listed in Appendix A.

The prediction from Simonin's model is compared with DNS for this simple test case. The principal result from DNS experiments is that the energy in both phases decreases monotonically. The net effect of the particles is to reduce fluid energy, and this effect grows with increasing Stokes numbers. The prediction from Simonin's model is that the TKE in the fluid phase decreases monotonically, but the net effect of particle to reduce fluid energy *decreases* with increasing Stokes numbers, which is opposite to DNS results. See Fig. 5.1.

The model results for particle energy evolutions show steep decay at the beginning, which could also be found in the fluid energy decay. The particle energy decays monotonically and the decay of particle energy is observed to increase with the growth of Stokes numbers, which is consistent with the DNS data. See Fig. 5.2.

From the governing equation 3.1 in Chapter 3, the decay time scale of k_f and k_p could be defined as $k_f/\frac{dk_f}{dt}$ and $k_p/\frac{dk_p}{dt}$, and the governing equations for the reciprocals of these two time scales are

$$\begin{aligned}
\frac{1}{k_f}\frac{dk_f}{dt} &= \frac{1}{\alpha_f \rho_f k_f}\left\langle u_i''^{(f)} \frac{\partial\left(I_f \tau_{ki}\right)}{\partial x_k}\right\rangle + \frac{1}{\alpha_f \rho_f k_f}\left\langle u_i''^{(f)} S_{Mi}^{(f)}\right\rangle \\
\frac{1}{k_p}\frac{dk_p}{dt} &= \frac{1}{\alpha_p \rho_p k_p}\left\langle u_i''^{(p)} S_{Mi}^{(p)}\right\rangle .
\end{aligned} \tag{5.1}$$

The k_f equation in Simonin's model can be revised in terms of the reciprocal of the decay time scale for k_f, which is

$$\frac{1}{k_f}\frac{dk_f}{dt} = \frac{\Pi_{k_f}}{\alpha_f \rho_f k_f} - \frac{\varepsilon_f}{k_f} = \frac{\phi}{\tau_{12}^F}\left[\rho_{fp}\sqrt{\frac{k_p}{k_f}} - 2\right] - \frac{1}{\tau} \tag{5.2}$$

where ϕ is the mass loading and τ_{12}^F is the particle response time. In the budget plot of this equation, see Fig. 5.3, the decay of interphase TKE transfer contributes around 50% to the right hand side of Eq. 5.2. The particle response time τ_{12}^F is actually the time scale for interphase TKE transfer. As the particle Reynolds number Re_p based on $\langle|\bar{v}_r|\rangle_2$ is around unity, the expression for τ_{12}^F is simplified to,

$$\tau_{12}^F = \frac{4}{3}\frac{\bar{d}}{C_D\langle|\bar{v}_r|\rangle}\frac{\rho_p}{\rho_f} = \frac{4}{3}\frac{\alpha_f\bar{d}^2}{C_D Re_p \nu_f}\frac{\rho_p}{\rho_f} \approx \frac{\alpha_f\bar{d}^2}{18\nu_f}\frac{\rho_p}{\rho_f} \tag{5.3}$$

as $Re_p \approx 1$, the product of C_D and Re_p can be approximated by 24. Hence, in this homogeneous turbulent flow, under the conditions of all the Re_p approximating to 1, the particle response time is approximately constant during the evolution, and can be simplified to $\frac{\alpha_f d^2}{18\nu_f}\frac{\rho_f}{\rho_p}$ in Eq. 5.3.

The governing equation for k_p is also revised here as

$$\frac{1}{k_p}\frac{dk_p}{dt} = -\frac{1}{\tau_{12}^F}\left[2 - \rho_{fp}\sqrt{\frac{k_f}{k_p}}\right]. \tag{5.4}$$

The decay of k_p totally depends on the particle response time τ_{12}^F in Eq. 5.4. The sharp decay of k_p at the beginning time is mostly caused by this time scale. Hence it is clear that the particle response time cannot be used as the time scale for the TKE decay in fluid and particle phase.

The physical reason behind these anomalous behavior of k_f evolution with different particle Stokes number and also the steep decay of k_p at the beginning is because the particle response time, which is taken to be the interphase TKE transfer time scale, could be an appropriate time scale only for some specific range of particle–eddy interactions. In reality, particle turbulence interaction is a complex multiscale process. Even for the monodispersed gas–solid two phase flow, particles interact with a range of eddies with different length and time scales. Furthermore, the particle response time and the Stokes number for each particle is different, since each particle has a different instantaneous velocity. The particle response time defined here can only represent the characteristic time scale of particles interacting with the eddies in the dissipation range.

The reason for this discrepancy also lies in the fundamental inability of the Eulerian–Eulerian approach to describe the multiple time and length scales encountered in two–phase turbulent flows. In Eulerian–Eulerian models, all the quantities in the governing equations are averaged. These averaged time and length scales can only be valid for a range of time and length scales, if not properly modeled.

It is discussed in Chapter 4 that k_{fp} or ρ_{fp} is a pseudo–flow quantity. In Fig. 5.4, the particle energy decays even faster at the beginning, as $\rho_{fp}(0)$ decreases from 2.0 to 0.0. The model results show strong dependence on the pseudo–flow quantities like k_{fp} or ρ_{fp}, which reduces applicability of this model.

Particle–laden Homogeneous Shear Flow

In the DNS data for homogeneous shear flows by Elghobashi [20], for mass loading $\phi = 1.0$ and particle response time $\tau_p = 1.0$, the velocity covariance in fluid phase $\langle u''_{f,1} u''_{f,3} \rangle$ is reported. Since this term determined the production in the second moment equations Eq. 3.7, the detailed comparison is done for this case.[1] The results from Simonin's model are compared in Fig. 5.5. The reduction rate of k_f is much faster than DNS results, which is up to 70% off at $T = 3$.

The budget for this case in Fig. 5.6 shows that the interphase TKE transfer term is dominant and contributes most to the fast decay at the beginning. In Fig. 5.6, the comparison of the shear production shows a large difference between the DNS and model results. However, more appropriate comparison should be ρ_{f13}

$$\rho_{f13} = \frac{\langle u''_{f,1} u''_{f,3} \rangle}{\sqrt{\langle u''_{f1} u''_{f1} \rangle \langle u''_{f3} u''_{f3} \rangle}}, \tag{5.5}$$

and this is shown in Fig. 5.7. There is large difference at the beginning of evolution and after $T = 4$, the difference is small. This could be due to the initial conditions and also the interphase TKE transfer term.

The particle inertia study is done in the DNS study. Four different cases with the same mass loading $\phi = 0.1$ and $\tau_p = 0.1$, 0.25, 0.5, 1.0 shows increasing decaying rate with growth of

[1] The initial conditions is described in Appendix B.

particle response time. The comparison between DNS and model results is shown in Fig. 5.8. DNS data show that with increasing particle response time, the reduction rate of k_f increases. However, the results from Simonin's model give opposite trend with increasing particle response time.

Compared with DNS data for homogeneous shear flows, Simonin's model predicts the steep decay of fluid energy at the beginning of evolution. With increasing particle response time but fixed mass loading ϕ, Simonin's mode predicts the opposite trend for fluid energy decay as compared to DNS results.

5.2 Predictions of Ahmadi's Model

In this section, the model predictions from Ahmadi's model for particle–laden isotropic flows are compared with DNS data.

Decaying Homogeneous Turbulent Flows

Ahmadi's model shows good agreement of DNS results for evolution of fluid energy, except for some quantitative difference after $t/Te = 1.5$. The decay of k_f is not enough after $t/T_e = 1.5$. This is because of the simple algebraic closure that is used for the dissipation rate in the fluid energy. The anomalous variation of fluid energy evolution with different particle Stokes number has not been found in Ahmadi's model. See Fig. 5.9.

To analyze the governing equation in Ahmadi's model, k_f equation is rewritten in term of reciprocal of decay time scale.

$$\frac{1}{k_f}\frac{dk_f}{dt} = \frac{2D_0}{\alpha_p\rho_p}\phi\left(\frac{k_p}{k_f} - c\right) - \frac{\varepsilon_f}{k_f}$$

where ϕ is the mass loading and $\frac{D_0}{\alpha_p\rho_p}$ is the particle response frequency in this model, which can be further simplified as

$$\frac{D_0}{\alpha_p\rho_p} = \frac{18\nu_f}{\bar{d}^2}\frac{\rho_f}{\rho_p}\frac{1}{\left(1-\frac{\alpha_p}{\nu_m}\right)^{0.25\nu_m}} \approx \frac{18\nu_f}{\bar{d}^2}\frac{\rho_f}{\rho_p} \quad \text{where } \alpha_p \ll 1 \tag{5.7}$$

In the definition of c, since $\frac{\alpha_p\rho_p}{D_0}$ is the particle response time in this model, c can be viewed as a function of the Stokes number, whose definition is based on Lagrangian time macroscale

of turbulence T_L. The particle response time does not change during the evolution, since the particle Reynolds number is based on mean slip velocity, which is always zero in this case.

In the model prediction of Ahmadi's model, very fast decay of k_p is observed in the evolution of the particle energy, and the quantitative discrepancy between model predictions and DNS data is quite large. See Fig. 5.10. The anomalous variation of k_p evolution with different particle Stokes numbers is not found in the model results.

If the governing equation of k_p is rewritten in terms of the reciprocal of the TKE decay time scale, it is obvious that the decay time scale of k_p is determined by the particle response time. The model equation for decay frequency of k_p is

$$\frac{1}{k_p}\frac{dk_p}{dt} = \frac{2D_0}{\alpha_p \rho_p}\left[c\frac{k_f}{k_p} - 1\right] = 2\frac{D_0}{\alpha_p \rho_p}\left[c\frac{k_f}{k_p} - 1\right] \tag{5.8}$$

The principal time scale used to model the interphase transfer of TKE between k_f and k_p is the particle response time τ_{12}^F. For the reason noted in the previous section, this time scale is not an appropriate time scale for interphase TKE transfer.

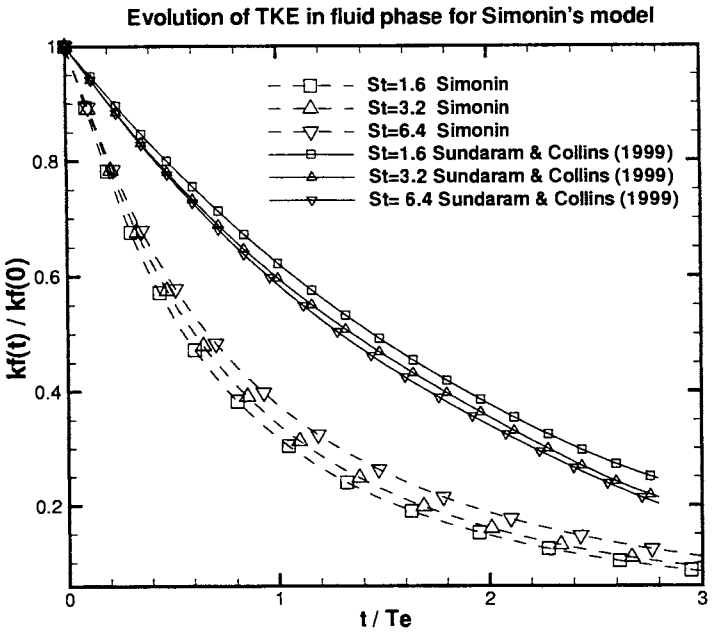

Figure 5.1 Evolution of normalized TKE in fluid phase for Simonin's model and compared with DNS data for particle-laden decaying homogeneous turbulence. The simulation time is scaled by the initial large eddy turnover time $T_e(0)$ from DNS. (Hereafter the simulation time in the model predictions for particle-laden isotropic turbulence is scaled by $T_e(0)$.)

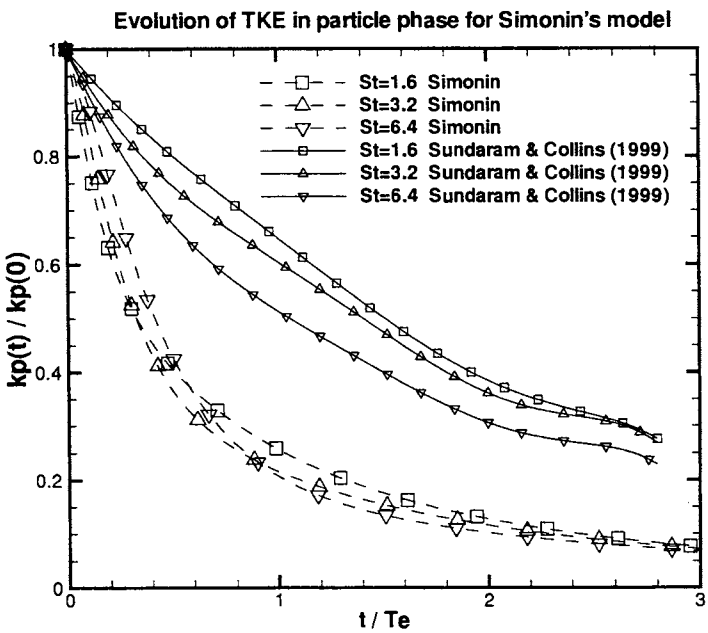

Figure 5.2 Evolution of normalized TKE in particle phase for Simonin's model and comparison of model results with DNS data for particle-laden decaying homogeneous turbulence.

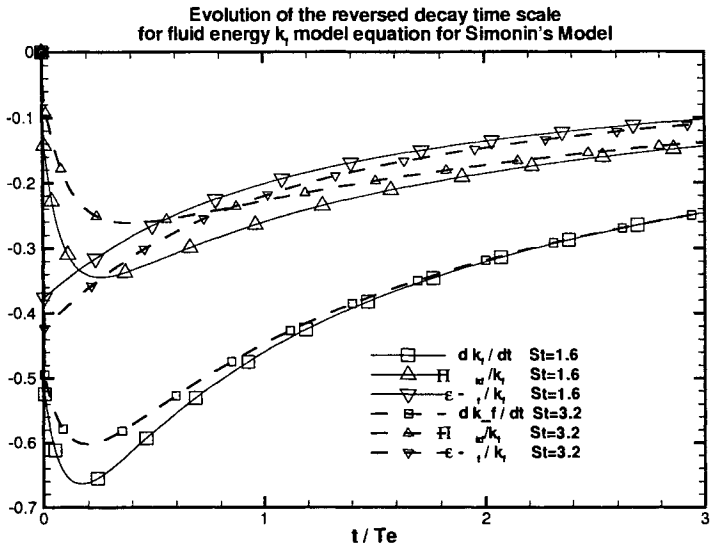

Figure 5.3 Evolution of inverse decay time scale in the modeled equation for fluid phase TKE from Simonin's model for particle–laden decaying homogeneous turbulence. The quantity ε_f/k_f is actually the eddy turnover frequency $1/\tau$ in Simonin's Model. Results for $St = 1.6$ and $St = 3.2$ are listed here for comparison.

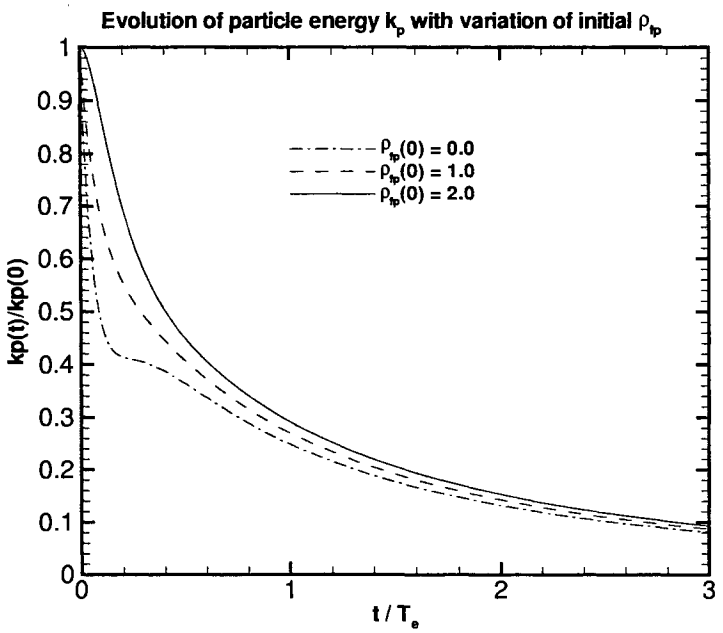

Figure 5.4 Evolution of TKE in particle phase with different initial ρ_{fp} for Simonin's model for particle–laden decaying homogeneous turbulence. The case shown here is for St=1.6.

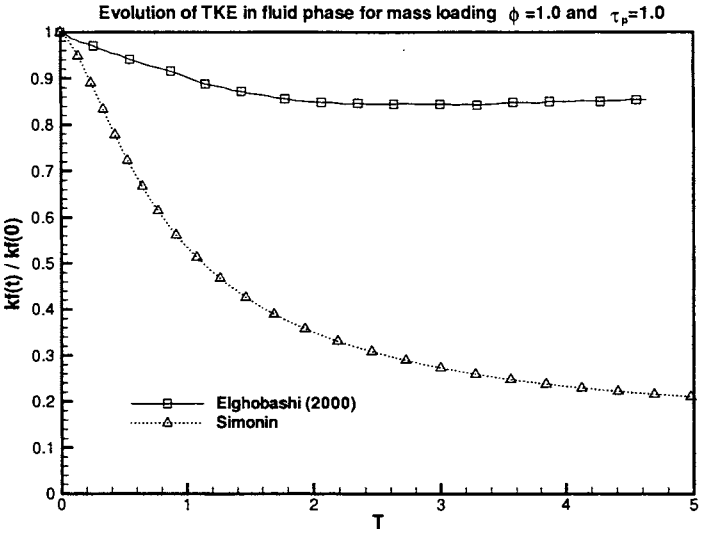

Figure 5.5 Evolution of fluid energy from predictions of Simonin's model for particle–laden homogeneous shear flow.

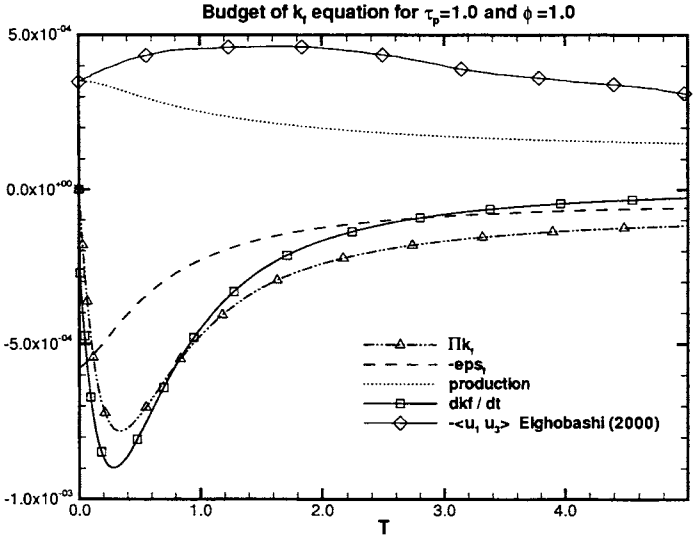

Figure 5.6 Budget plot of fluid energy from Simonin's model equations for particle–laden homogeneous shear flow.

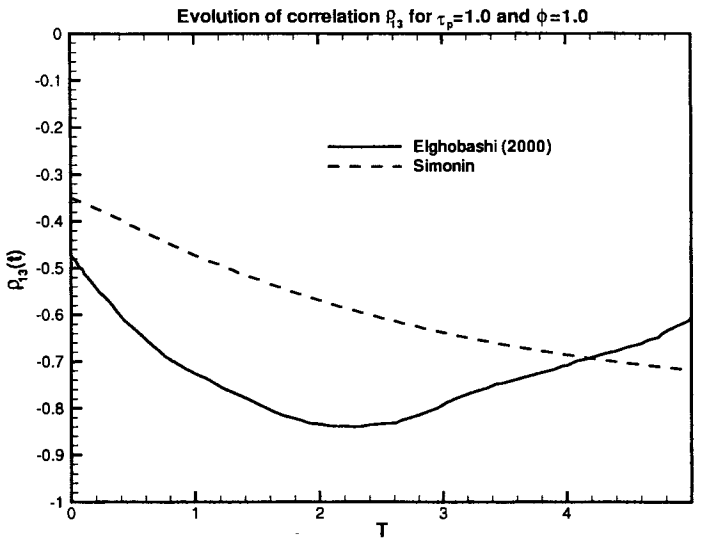

Figure 5.7 Evolution of the velocity correlation ρ_{f13} from Simonin's model for particle–laden homogeneous shear flows.

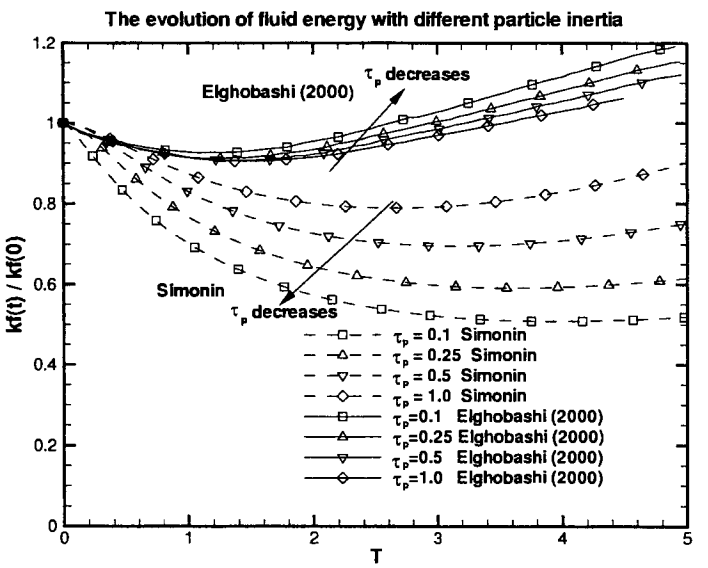

Figure 5.8 Evolution of fluid energy for different particle response time τ_p and the same mass loading ϕ for particle–laden homogeneous shear flows.

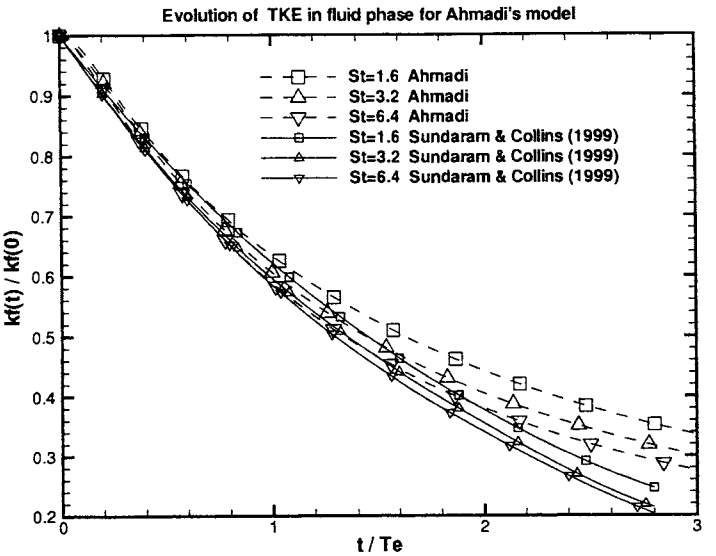

Figure 5.9 Evolution of normalized TKE in fluid phase for Ahmadi's model and comparison of model results with DNS data for particle–laden decaying homogeneous turbulence.

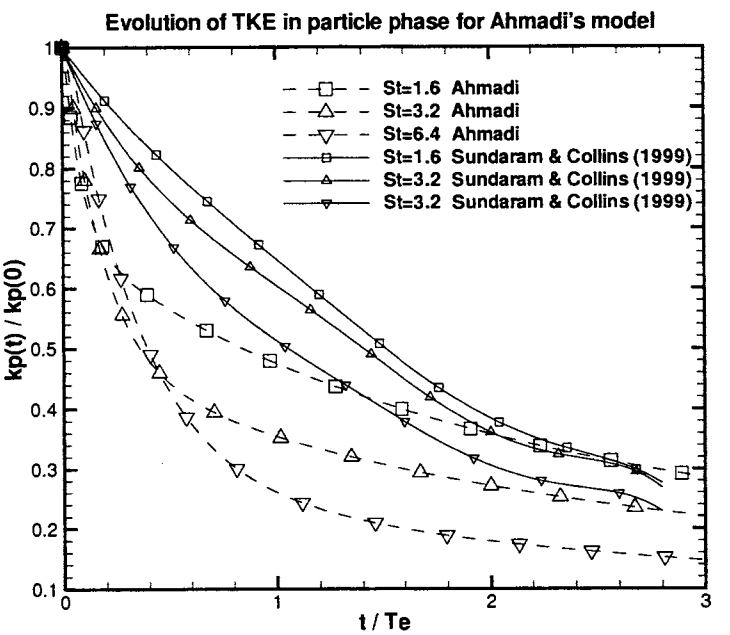

Figure 5.10 Evolution of normalized TKE in particle phase for Ahmadi's model and comparison of model results with DNS data for particle–laden decaying homogeneous turbulence.

CHAPTER 6. THE EQUILIBRATION OF ENERGY MODEL

As it is discussed in Chapter 5, the model predictions from Simonin and Ahmadi's model show fast decay at the beginning of the particle energy evolution. For Simonin's model, the decay rate of TKE in fluid phase shows opposite trends with the growth of particle response time when compared with DNS results for particle–laden decaying homogeneous turbulence and homogeneous shear flows.

A new multiphase model, Equilibration of Energy Model (EEM), is proposed in this chapter, which has a new time scale for interphase TKE transfer for dilute particle–laden turbulent flows. Model predictions from EEM and are carefully evaluated and compared with DNS results for particle-laden isotropic turbulence [1] and particle–laden homogeneous shear flows [20]. The multiscale interaction time scale is also incorporated in Simonin and Ahmadi's models, and this improves the performance of these two models.

6.1 Multiscale Interaction Model

In this section, a new time scale is proposed to model the interphase TKE transfer. This new time scale is implemented in both Simonin and Ahmadi's models, which improves the model performance for the particle–laden isotropic turbulence.

The anomalous model behavior of k_f with different Stokes number in Simonin's model predictions and the sharp decay of k_p in predictions from both models need to be improved. In the two models tested, the complex particle–fluid interaction is characterized by a single time scale, the particle response time τ_p. However, in the governing equation of both DNS studies [1, 20], the particle response time is used as the principal time scale in the interphase momentum and energy transfer. In the DNS study, the particles interact with a range of

time and length scales in the flow, the energy containing range, the inertial range and the dissipation range, which is a more realistic implementation of fluid–particle interactions. Based on this understanding, a multiscale interaction model was first proposed by Pai et. al. [30], to improve the multiphase turbulence model in KIVA, which is based on the Lagrangian–Eulerian approach. This multiscale interaction model is implemented in the Eulerian–Eulerian models tested in this work.

One can define a particle Stokes number based on τ_l, a characteristic eddy time scale, rather than the Kolmogorov time scale. τ_l is defined as follows,

$$\tau_l = \frac{l}{|\mathbf{u}_g'|} = \frac{|\mathbf{u}_g'|^2}{\varepsilon_f}$$

where l is the size of some eddy, and $|\mathbf{u}_g'|$ is assumed to be joint–normal for the isotropic turbulence. Furthermore St_l can be scaled as

$$St_l = \frac{\tau_p}{\tau_l} \sim \frac{1}{|\mathbf{u}_g'|^2}$$

This means that more energetic eddies can be associated with a small Stokes number and small fluctuations can be associated with a large Stokes number. So corresponding to different size of eddies, there are different particle Stokes numbers.

The hypothesis is that for $St_l < 1$, the particle responds immediately to the flow. When particles are entrained in the eddies with $St_l < 1$, the particles will basically follow the characteristic time scale of the eddies. As St_l approaches 0, the particles follow the eddy turnover time.

For $St_l > 1$, the particle responds slowly to the flow. In this case, the characteristic size of the eddies is small and also $|\mathbf{u}_g'|^2$ is very small. Particles will not be entrained and will not move along with these small eddies. The inertia of the particle plays the important role when the particle interacts with small size eddies. Since the particle response time is a measure of the particle inertia, which depends on the density and the size of the particles, the particle follows its response time when $St_l > 1$.

For the two test cases, isotropic turbulence and homogeneous shear turbulence, the fluctuating velocity in the fluid phase is assumed to be joint normal, and the distribution of $|\mathbf{u}_g'|$ follows

the distribution like

$$f_Z(Z) = \sqrt{\frac{2}{\pi}} \frac{1}{\sigma_f^3} z^2 e^{-z^2/2\sigma_f^2}$$

where $Z = |\mathbf{u}'_g|$ and σ_f is the standard deviation of $|\mathbf{u}'_g|$, which is $\sqrt{\frac{2}{3}k_f}$. Figure 6.1 is the sketch of the distribution function of $|\mathbf{u}'_g|$. Following this hypothesis, the axis of $|\mathbf{u}'_g|$ will be split into two parts, and the transition fluctuating fluid velocity is called $|\mathbf{u}'_g|^*$ in this work. At $|\mathbf{u}'_g|^*$, $St_l = \tau_p/\tau_l$ is equal to 1.

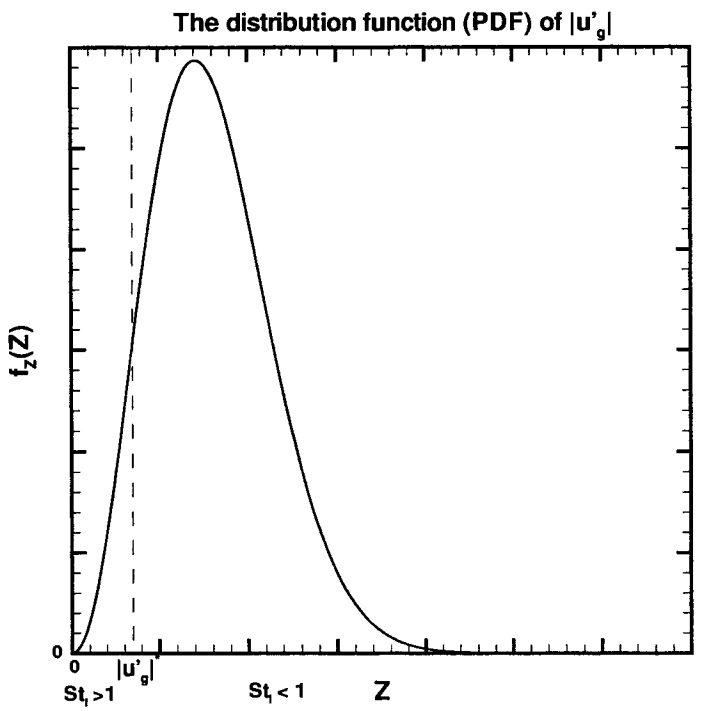

Figure 6.1 Sketch of the distribution function of $|\mathbf{u}'_g|$, where $Z = |\mathbf{u}'_g|$.

To construct a multiscale interaction time scale τ_i, the concept of the expected value or mean of a function is used here. The interaction time τ_i is a function of $|\mathbf{u}'_g|$, which is a random variable following the distribution function $f_Z(Z)$ in the test cases. It is hypothesized in this study that the interaction time is the unconditional mean of the interaction time τ_i weighted according to the probability function of $|\mathbf{u}'_g|$.

$$\langle \tau_i \rangle = \int_0^\infty \tau_i|_{Z=z} f_Z(Z) dZ$$

The function of τ_i is assumed to be

$$\tau_i = \tau_p \qquad 0 < |\mathbf{u}_g'| < |\mathbf{u}_g'|^* \tag{6.1}$$

$$\tau_i = St_l \cdot (\tau_p - \tau) + \tau \qquad |\mathbf{u}_g'|^* < |\mathbf{u}_g'| < \infty \tag{6.2}$$

The interaction time in the range $|\mathbf{u}_g'|^* < |\mathbf{u}_g'| < \infty$ is simply modeled as a linear function of St_l. As $St_l \to 0$, τ_i is equal to eddy turnover time τ and the particle just moves with the eddies. When $St_l \geq 1$, the particle responds slowly to the flow, and the particle response time τ_p is dominant here.

One can retrieve Simonin and Ahmadi's model from the expression of $\langle \tau_i \rangle$ by moving $|\mathbf{u}_g'|^*$ to infinity and $\langle \tau_i \rangle_{|\mathbf{u}_g'|^* \to \infty} = \tau_p$, where τ_p is the particle response time. This means that the particle responds to the flow at the particle response time scale for the entire range of $\mathbf{u}_g'$. If $|\mathbf{u}_g'|^*$ is moved to 0, all the particles respond to the surrounding fluid at the characteristic time scale of eddies.

The unconditional mean of τ_i is defined as

$$\langle \tau_i \rangle = \int_0^{|\mathbf{u}_g'|^*} \tau_p f_Z(Z) dZ + \int_{|\mathbf{u}_g'|^*}^{\infty} [St_l \cdot (\tau_p - \tau) + \tau] \cdot f_Z(Z) dZ \tag{6.3}$$

where $f_Z(Z)$ is the distribution function of $|\mathbf{u}_g'|$.

After implementing the new multiscale interaction model in Simonin's model, the steep decay at the beginning of k_f and k_p evolution is removed for particle–laden decaying homogeneous turbulence. The incorrect trend of k_f decaying rate with increasing particle Stokes number is corrected with implementation of $\langle \tau_i \rangle$ in Simonin's model as interphase TKE transfer time scale (See Fig. 6.2, Fig. 6.3).

For particle–laden homogeneous shear flows, results from Simonin's model with $\langle \tau_i \rangle$ become closer to DNS data from Elghobashi for special case mass loading $\phi = 1.0$ and particle response time $\tau_p = 1.0$, see Fig. 6.8. For the fluid energy evolution with increasing particle response time $\tau_p = 0.1, 0.25, 0.5, 1.0$, incorrect trend with increasing Stokes number in Simonin's model results is corrected after implementing $\langle \tau_i \rangle$ as the interphase TKE transfer time scale, see Fig. 6.4.

For Ahmadi's model, the fast decay of particle energy at the beginning is eliminated after the implementation of $\langle \tau_i \rangle$ in Ahmadi's model. See Fig. 6.5. The idea of multiscale interaction time scale improves the performance of both Simonin and Ahmadi's models for particle–laden isotropic turbulence in this study.

6.2 Equilibration of Energy Model

In this section, a new multiphase model based on the multiscale interaction model is proposed and tested in the isotropic particle–laden turbulent flow and the particle–laden homogeneous turbulent shear flow.

6.2.1 Description of EEM

The two turbulence models tested for particle–laden flow use the particle response time τ_p as the time scale for interphase turbulence kinetic energy transfer. In Simonin's model, the pseudo–flow quantity k_{fp} is used to account for the fluid–particle velocity covariance. Ahmadi's model uses the single phase dissipation model for gas–solid two–phase flows. The predictions from both models show the considerable quantitative and qualitative difference when compared with DNS results for particle–laden isotropic turbulence.

A new model is proposed to use the interphase TKE transfer time scale τ_π, and is designed to be simple enough so as to be amenable to some analysis in the homogeneous case. This model is designed by considering the behavior of a two–phase flow system in the limit of stationary turbulence. It is proposed that if the fluid turbulence in a homogeneous particle–laden turbulent flow is forced to balance the dissipation, the particle phase TKE k_p and fluid energy k_f will evolve to their respective equilibrium values k_f^e and k_p^e over the interphase TKE transfer time scale τ_π.

The equilibration of energy concept can be extended to a corresponding multiphase turbulence model in the Lagrangian–Eulerian approach, as described in Pai & Subramaniam [30]. In that work, a system of coupled Langevin equations for the fluctuating velocity in each phase is proposed with drift and diffusion terms coupled through the interphase TKE transfer time

scale τ_π.

The model equations are written in terms of $e_f = \rho_f \alpha_f k_f$ and $e_p = \rho_p \alpha_p k_p$, which are the contributions to the total mixture energy $e_m = \rho_m k_m$ from each phase, where the mixture density $\rho_m = \rho_f \alpha_f + \rho_p \alpha_p$. The model equations for e_f and e_p are

$$\begin{aligned} \frac{de_f}{dt} &= -\frac{e_f - e_f^e}{\tau_\pi} - \rho_f \alpha_f \varepsilon_f \\ \frac{de_p}{dt} &= -\frac{e_p - e_p^e}{\tau_\pi} \end{aligned}$$

where the superscript e means the equilibrium state. Here the collisions are assumed to be elastic in the particle phase, thus the dissipation rate in the particle phase is zero.

The equilibrium values of fluid and particle phase energy ($e_f^e = \rho_f \alpha_f k_f^e$ and $e_p^e = \rho_p \alpha_p k_p^e$), are determined by a model constant C_2 which is defined as

$$C_2 = \frac{e_p^e}{e_m}, \quad 1 - C_2 = \frac{e_f^e}{e_m}$$

where C_2 lies between 0 and 1. The model parameter C_2 is the fraction of the specific mixture energy presented in the particle phase at equilibrium, and it is assumed to be independent of time, since it is defined at a stationary state. C_2 still can be a function of the parameters like mass loading ratio ϕ. In the decaying case, the equilibrium values e_f^e and e_p^e can change with time, because the total fluctuating velocity energy changes, but C_2 is a model constant and that does not change with time.

The dissipation rate of fluid energy is modeled as

$$\alpha_f \rho_f \frac{d\varepsilon_f}{dt} = -C_{\varepsilon,3} \frac{\varepsilon_f}{k_f} \cdot \left(\frac{e_f - e_f^e}{\langle \tau_i \rangle} \right) - C_{\varepsilon,2} \alpha_f \rho_f \frac{\varepsilon_f^2}{k_f} \tag{6.4}$$

The dissipation rate model in EEM is formulated after the dissipation rate mode equation in Simonin's model. In particle–laden turbulent flows, the particle wake and boundary layer can enhance the decay of TKE in the whole system, which is described by the first term on right hand side of Eq. 6.4. The dissipation caused by the viscous effects is described in the second term.

The interphase TKE transfer time scale τ_π is assumed to be a function of $\langle \tau_i \rangle$ discussed in Section 6.1

$$\tau_\pi = \frac{\langle \tau_i \rangle}{C_\pi} \quad \text{or} \quad C_\pi = \frac{\langle \tau_i \rangle}{\tau_\pi} \tag{6.5}$$

where $\langle \tau_i \rangle$ is the multiscale interaction time scale.

Then for particle–laden isotropic turbulence, the equation system for EEM is

$$\frac{dk_f}{dt} = -\frac{1}{\tau_\pi}\left[C_2 k_f - (1 - C_2)\phi k_p\right] - \varepsilon_f \tag{6.6}$$

$$\frac{d\varepsilon_f}{dt} = -C_{\varepsilon,3}\frac{\varepsilon_f}{k_f}\frac{1}{\tau_\pi}\left[C_2 k_f - (1 - C_2)\phi k_p\right] - C_{\varepsilon,2}\frac{\varepsilon_f^2}{k_f} \tag{6.7}$$

$$\frac{dk_p}{dt} = -\frac{1}{\tau_\pi}\left[(1 - C_2)k_p - \frac{C_2}{\phi}k_f\right] \tag{6.8}$$

where $\phi = \alpha_p \rho_p / (\alpha_f \rho_f)$ is the mass loading ratio.

The proposed model requires specification of the two model constants C_2 and C_π. In the absence of the relevant results from DNS of stationary turbulence, it is hypothesized that C_2 likely has a strong dependence on the mass loading ϕ of the system, and it is also hypothesized that C_2 is likely to not likely depend strongly on the volume fraction α_p for dilute flows, or particle Reynolds number in the Stokes regime, or particle Stokes number St. In this study, C_2 is chosen to be a linear function of mass loading ϕ, and C_2 can be chosen around 0.6ϕ. The interphase TKE transfer time scale has been discussed and verified in the previous section. C_π is chosen to be $2 \sim 3$.

EEM is similar to Ahmadi's model, however, to compared with Ahmadi's model, EEM has clear physical meaning and the model coefficients can be extracted from detailed DNS studies of the particle–laden stationary turbulent flows. Furthermore, EEM has no unclosed model parameters.

For particle-laden homogeneous shear turbulence, the production due to the homogeneous shear will take effect. In EEM, the concept of turbulent eddy–viscosity is used to model the production due to the shear. The simplified governing equations for the homogeneous shear

flows are

$$\frac{dk_f}{dt} = \Pi_{k_f} - \varepsilon_f - \langle u''_{f,1}u''_{f,3}\rangle \frac{\partial U_{f,1}}{\partial x_3} \tag{6.9}$$

$$\frac{d\varepsilon_f}{dt} = \Pi_{\varepsilon_f} - \frac{\varepsilon_f}{k_f}\left[C_{\varepsilon,1}\langle u''_{f,i}u''_{f,j}\rangle \frac{\partial U_{f,i}}{\partial x_j} + C_{\varepsilon,2}\varepsilon_f\right] \tag{6.10}$$

$$\frac{dk_p}{dt} = \Pi_{k_p} - \langle u''_{p,1}u''_{p,3}\rangle \frac{\partial U_{p,1}}{\partial x_3} \tag{6.11}$$

where Π_{k_f}, Π_{ε_f} and Π_{k_p} represent the interphase TKE transfer. The velocity correlation in the fluid phase $\langle u''_{f,1}u''_{f,3}\rangle$ is modeled through the concept of turbulent eddy viscosity, and is the same as that in the single turbulence model

$$\langle u''_{f,1}u''_{f,3}\rangle = -\nu_f^t \frac{\partial U_{f,1}}{\partial x_3} \qquad \text{where} \quad \nu_f^t = C_\mu \frac{k_f^2}{\varepsilon_f} \tag{6.12}$$

where $C_\mu = 0.09$. The velocity correlation in particle phase $\langle u''_{p,1}u''_{p,3}\rangle$ is modeled as

$$\langle u''_{p,1}u''_{p,3}\rangle = -\nu_p^t \frac{\partial U_{p,1}}{\partial x_3} \qquad \text{where} \qquad \nu_p^t = C_{\mu 2} k_p \langle \tau_i \rangle \tag{6.13}$$

where $C_{\mu 2}$ is chosen to be $0.001 \sim 0.003$ in this case. For relatively dense collision–dominated mixtures, the turbulent viscosity in the particle is modeled as $\nu_p^t = C_{\mu 2}\alpha_p d(k_p)^{1/2}$, where $C_{\mu 2}$ is a function of particle volume fraction and d is the mean diameter of particle phase [7, 8]. For dilute mixtures, the fluid turbulence dominates and the particles are transported by the fluid motion. It is suggested [7] that the fluid length scale should be the relevant scale in ν_p^t. In EEM, the multiscale interaction time $\langle \tau_i \rangle$ has the fluid phase turbulence information in it and this makes it the appropriate scale to model the dilute mixture. The model coefficients in EEM are listed in Table 6.1

Table 6.1 List of coefficients for EEM

C_2	$C_{\varepsilon,2}$	$C_{\varepsilon,3}$	C_π	$C_{\mu 2}$
0.6ϕ	1.92	1.2	$2.0 \sim 3.0$	$0.001 \sim 0.003$

6.2.2 Model Predictions of EEM for two canonical test cases

In this section, the model predictions from EEM for particle–laden decaying homogeneous turbulence and particle–laden homogeneous shear flows are described. The predictions from

EEM for decaying turbulence are shown in Fig. 6.6 and 6.7. The model results match the fluid phase dissipation quite well at the beginning of the evolution, and small quantitative discrepancy is observed after $t/T_e > 1.5$. EEM can reproduce the trend of the fluid energy k_f decay rate with increasing Stokes numbers correctly. The decay in particle energy is a little smaller than the DNS results, but the overall trend is quite good.

For particle–laden homogeneous shear flows, predictions from EEM are compared with those from Simonin's model and Simonin's model improved with multiscale interaction time scale $\langle \tau_i \rangle$. For mass loading $\phi = 1.0$ and particle response time $\tau_p = 1.0$, the velocity covariance $\langle u''_{f,1} u''_{f,3} \rangle$ is reported. Since this term determines the production in the second moment equations, the detailed comparison is done. In Fig. 6.8, the fluid energy evolution from EEM is quite close to the DNS results at the beginning ($T < 1$). But after $T > 1$, the fluid energy start to increase, which is different from the DNS results. Here the model coefficient C_2 is chosen to be 0.5, since C_2 is suggested to be around 0.6ϕ Compared with model predictions from Simonin's model and Simonin's model improved with $\langle \tau_i \rangle$, EEM predicts stronger production in fluid phase.

From the budget plot Fig. 6.10, it is the balance of production and dissipation that determines the evolution of fluid energy. The evolution of dissipation in fluid phase is reported in DNS data. If the modeled dissipation is replaced with the dissipation rate in fluid phase from DNS study, the increase in fluid energy will be eliminated. Furthermore by increasing $C_{\mu 2}$ in particle phase shear production, the fluid energy increases and with $C_{\mu 2} = 0.5 \sim 0.8$, the model prediction from EEM is quite close to DNS results, see Fig. 6.11. From these, it can conclude that if the fluid dissipation can be modeled more accurately, the predictions from EEM can be further improved.

The correlation ρ_{13} of fluctuating velocity $u_{f,1}$ and $u_{f,3}$ is shown in Fig. 6.9. The results from EEM are closer to DNS data at the long time of simulations. The large discrepancy at the beginning of evolution observed in Simonin's model results predictions is also in EEM's results. This discrenpancy can be caused by the influence of initial conditions from DNS study.

The model results for particle inertia study from EEM are shown in Fig. 6.12. The results

from Simonin's model with multiscale interaction time scale are presented for comparison. The model results from EEM is very close to DNS data, and the trend with variation of particle inertia is correct. But the difference between different particle inertia is too small. One possible reason for this deficiency is that there is no particle inertia information in the fluid production term. One way to improve this is to use $\langle \tau_i \rangle$ as the time scale in ν_f^t instead of eddy turnover time τ. But without detailed DNS data for variation of shear production with different particle inertia, the model for fluid and particle shear production terms in EEM can not be specified with complete confidence.

6.2.3 Discussion

In previous section, a multiphase turbulence model, EEM, is proposed, which uses a new time scale $\langle \tau_i \rangle$ for interphase TKE transfer. This new time scale succeeds in reproducing the trend of fluid phase TKE decay rate with variation of particle Stokes numbers in the particle–laden isotropic turbulence. From Section 6.2, the EEM's predictions for homogeneous shear are not as good as expected. It is suggested that by improving the modeling of fluid dissipation, the model results can be further improved. However, the DNS study of Elghobashi [20] doesn't provide the detailed TKE budget study for k_f and k_p for various mass loading ϕ and particle Stokes numbers St. The production term in particle phase suggested in EEM has the appropriate time and length scale in it. Moreover, there is possibility that the model coefficients like $C_{\mu 2}$ are functions of particle Stokes number, particle Reynolds number and mass loading, but the further specification of model coefficients like $C_{\mu 2}$ needs more detailed DNS studies for particle–laden stationary turbulence.

The case of particle–laden stationary turbulence is important, since the statistically stationary flows can be evolved to an equilibrium in which particle motion, and the effect of particles on the flow, are independent of initial conditions. Furthermore, the time and length scale ratio of the turbulence relative to the particles also become stationary. The DNS results from statistically stationary flows will reveal useful information for modeling. Two test cases chosen in this work are for decaying turbulence, which brings some difficulties when identifying

and separating the influence from the initial conditions.

The dissipation in fluid phase is another important issue in DNS study of particle–laden turbulent flows. The DNS results for the two test cases are all based on the point particle assumption, which means that all the particles in the flow field are modeled as a point and the linear drag law is applied on each particle. The force of particle acting on the flow field is done by the "reverse" or "backward" interpolation functions. The flow field around the particle is not solved with this kind of method. To calculate the dissipation in fluid phase accurately, one needs to solve the flow field around each particle, which means that the computation will consume huge amount of computation power, which are becoming commonplace nowadays.

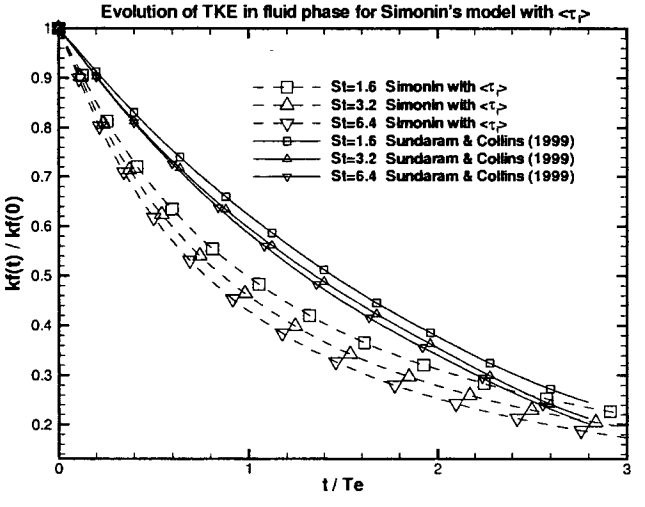

Figure 6.2 Evolution of normalized TKE in the fluid phase for Simonin's model incorporated with the multiscale interaction time scale $\langle \tau_i \rangle$ and comparison of model results with DNS data for particle–laden isotropic turbulence.

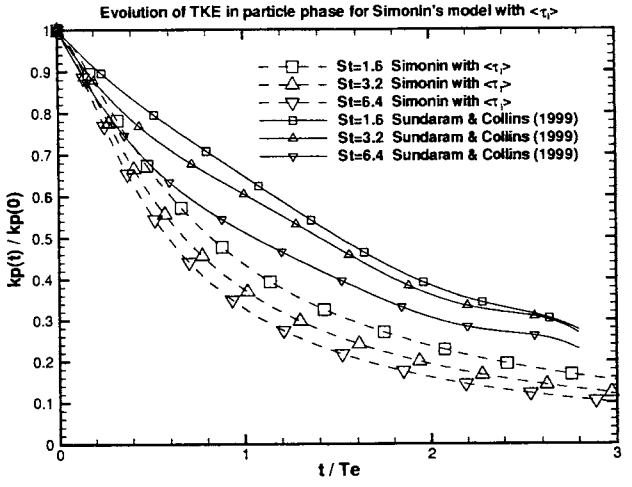

Figure 6.3 Evolution of normalized TKE in the particle phase for Simonin's model incorporated with the multiscale interaction time scale $\langle \tau_i \rangle$ and comparison of model results with DNS data for particle–laden isotropic turbulence.

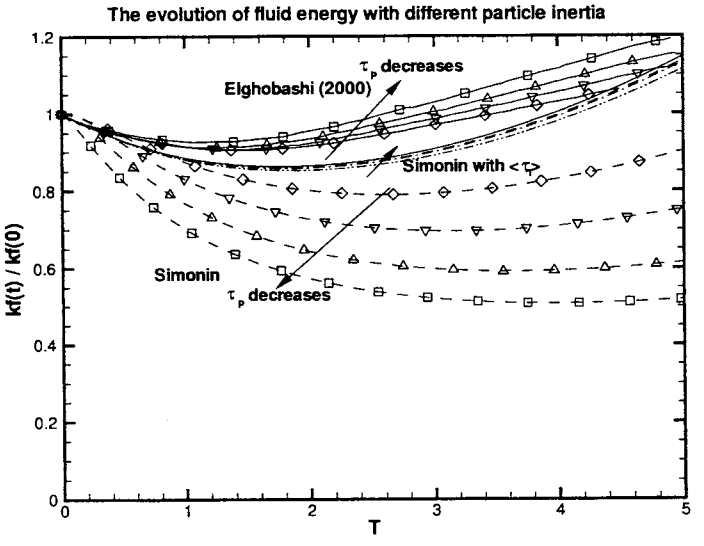

Figure 6.4 Evolution of the fluid energy for cases with different particle inertia and the same mass loading. $\square$ represents $\tau_p = 0.1$; $\triangle$ represents $\tau_p = 0.25$; $\triangledown$ represents $\tau_p = 0.5$; and $\Diamond$ represents $\tau = 1.0$.

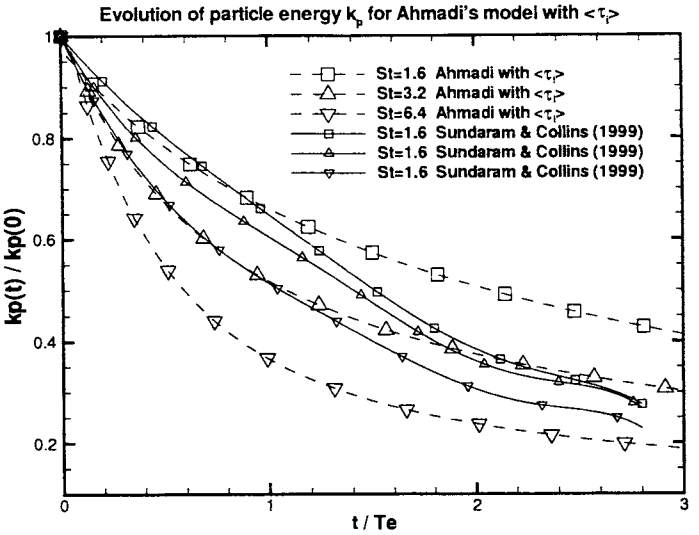

Figure 6.5 Evolution of normalized TKE in the particle phase for Ahmadi's model improved the multiscale interaction time scale $\langle \tau_i \rangle$ and comparison of model results with DNS data for particle–laden isotropic turbulence.

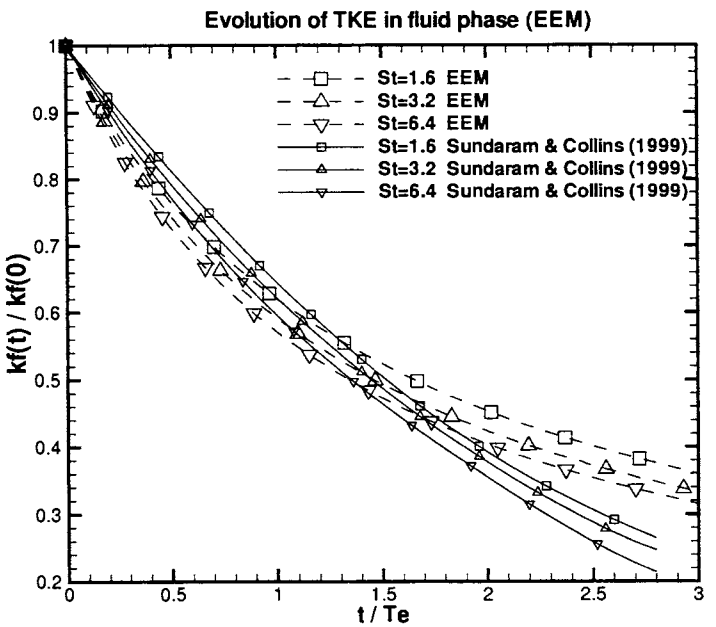

Figure 6.6 Evolution of normalized TKE in the fluid phase for EEM and compared with DNS data for particle–laden decaying homogeneous turbulence.

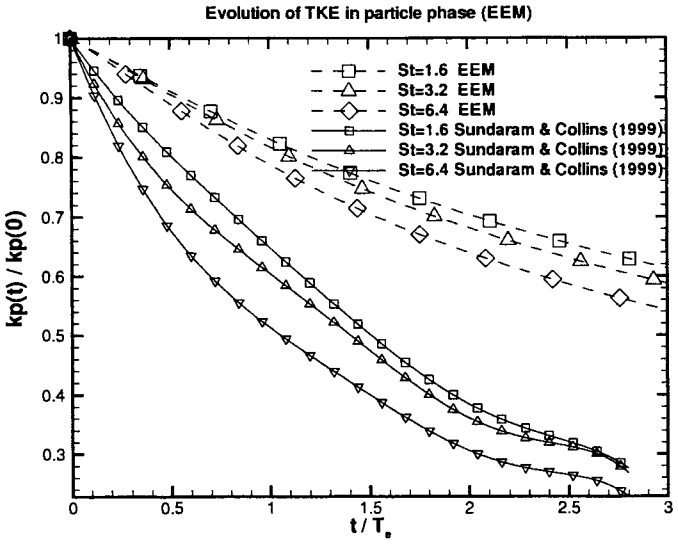

Figure 6.7 Evolution of normalized TKE in the particle phase for EEM and compared with DNS data particle–laden decaying homogeneous turbulence.

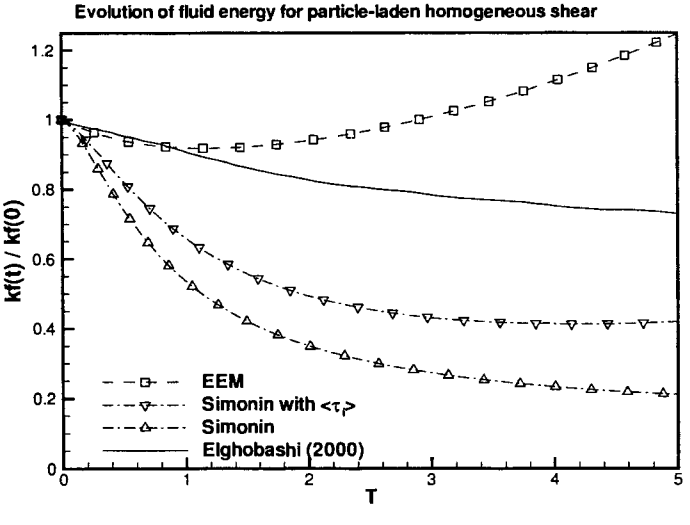

Figure 6.8 Evolution of normalized TKE in fluid phase for EEM, Simonin's model and Simonin's model with multiscale interaction time scale $\langle \tau_i \rangle$ for particle–laden homogeneous shear flows.

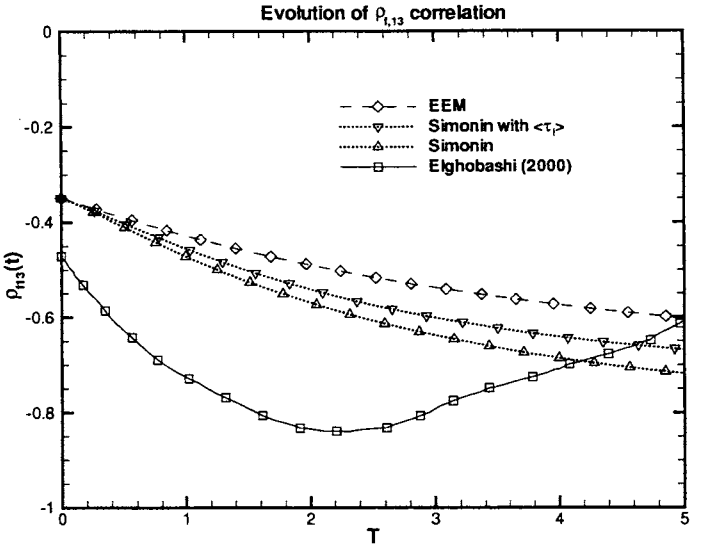

Figure 6.9 Evolution of the velocity correlation ρ_{f13} for EEM, Simonin's model and Simonin's model implemented with multiscale interaction time scale $\langle \tau_i \rangle$

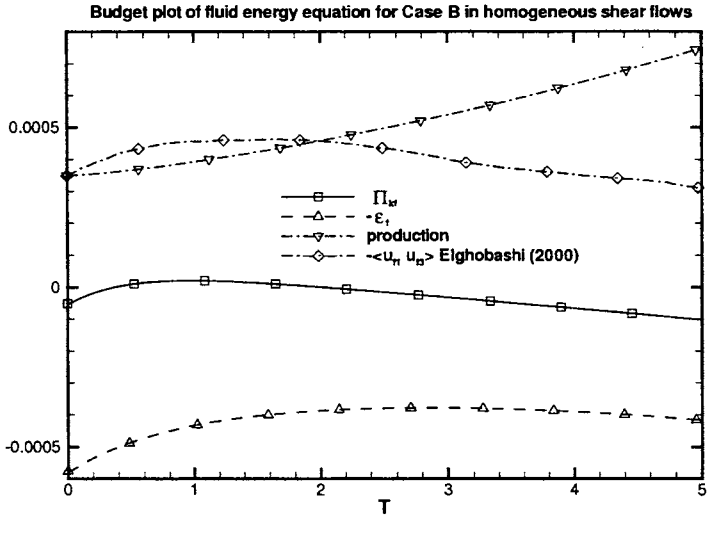

Figure 6.10 Budget plot for fluid energy equation of EEM for Case B in the particle-laden homogeneous shear flows.

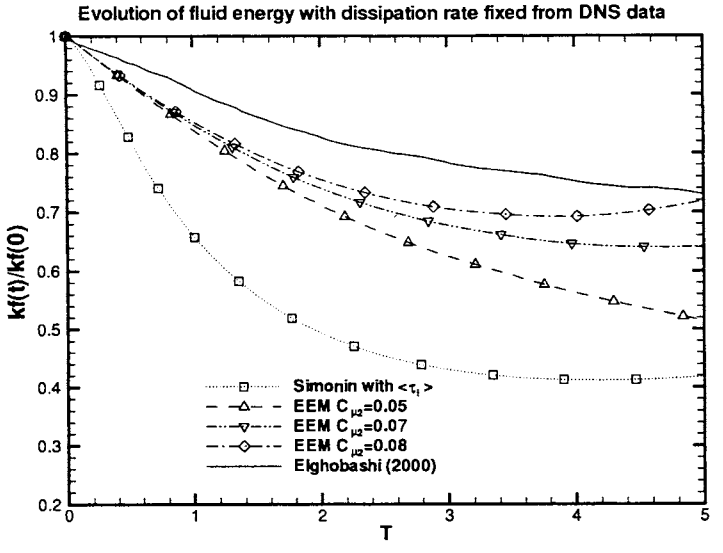

Figure 6.11 Evolution of TKE in fluid phase with fluid dissipation rate fixed from DNS data for EEM.

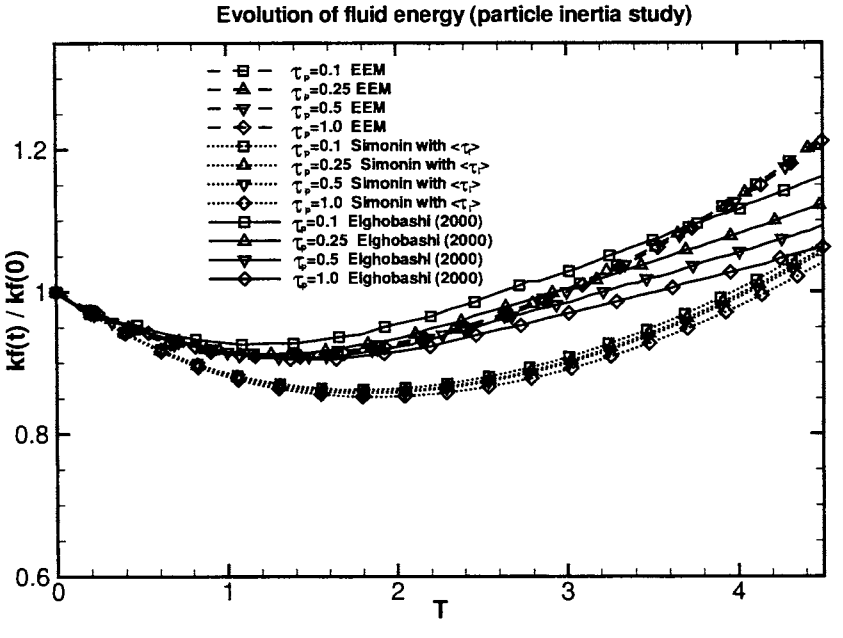

Figure 6.12 Evolution of the fluid energy for cases with different particle response time τ_p and the same mass loading $\phi = 0.1$.

CHAPTER 7. CONCLUDING REMARKS

Two multiphase turbulence models from Simonin [10, 11] and Ahmadi [7, 8]) are compared with direct numerical simulations (DNS) of two canonical flows: homogeneous, particle–laden isotropic turbulent flow [1], and particle–laden homogeneous shear flow [20]. The principal findings from this performance assessment of the two models are:

(1) For homogeneous particle–laden turbulent flow, both models predict a faster decay rate of fluctuating energy (in both phases) than found in the DNS. The reason for the faster decay is that the particle response time ($\tau_p = d^2\rho_p/18\mu_f$) is used as the time scale for interphase TKE transfer in both models. For monodisperse particles there is a single particle response time scale. The results indicate that a single particle response time does not adequately characterize the interaction between the particles and the range of turbulent eddy sizes, which is responsible for interphase TKE transfer.

(2) Anomalous variation of TKE with different particle Stokes numbers is found in the results. The interphase TKE transfer is the dominant term in Simonin's model that causes this anomalous model behavior. The interphase TKE transfer model introduces a pseudo–flow quantity k_{fp}, and uses the particle response time as the relevant time scale for interphase TKE transfer.

The following areas for model improvement are identified: (i) model for interphase TKE transfer, especially the time scale of interphase TKE transfer, and (ii) correct prediction of TKE evolution with variation of particle Stokes number. Furthermore, Ahmadi's model has an unclosed length scale associated with the model for fluid phase dissipation rate. In Simonin's model, a pseudo–flow quantity k_{fp} is introduced, and it is unclear how the initial and boundary conditions for this term should be specified. These deficiencies in Simonin and Ahmadi's model

limit the appliability of these two models.

A new multiphase turbulence model, Equilibration of Energy Model (EEM), is proposed in this paper. A noteworthy point of EEM is that a multiscale interaction time scale $\langle \tau_i \rangle$ is proposed to account for the interaction of particle with a range of eddy sizes (from the energy containing range to the dissipation range). As the particle Stokes number approaches zero, $\langle \tau_i \rangle$ approaches the eddy turnover time; and $\langle \tau_i \rangle$ approaches particle response time τ_p in the limit of $St \to \infty$.

This new time scale $\langle \tau_i \rangle$ is incorporated in the interphase TKE transfer terms of Simonin and Ahmadi's models. It is found that for particle–laden isotropic turbulence, the predicted decay of TKE at the beginning of simulation is improved. The anomalous variation of TKE with particle Stokes numbers in Simonin's model is also eliminated by using the time scale $\langle \tau_i \rangle$. The predictions from EEM shows good agreement with the DNS results for particle-laden isotropic turbulence.

For more complicated flow cases, like the particle–laden homogeneous shear flows, the model predictions can be further improved if the dissipation rate in fluid phase is modeled with more accuracy. A difficulty that is encountered in shear flows is that the detailed budget of terms in the TKE equation is not available from existing DNS studies.

Although EEM is a simple model, it has clear a physical interpretation and gives reasonable trends with the important nondimensional parameters of particle–laden turbulent flow. It can be a useful engineering tool for CFD simulation of particle–laden turbulent flows.

Future work is suggested as follows:

1) To model more complicated case, like inhomogeneous turbulent flow, the model for Reynolds stress in both phase is required.

2) For more realistic cases, such as turbulent pipe flows, the boundary conditions for both phases will be necessary.

3) The model coefficients in EEM need further specification. Then the detailed DNS study of particle–laden stationary turbulence is required.

BIBLIOGRAPHY

[1] S. Sundaram, Lance R. Collins. A numerical study of the modulation of isotropic turbulence by suspended particles. *J. Fluid Mech.*, 379(9):105–143, Sept. 1999.

[2] S. Subramaniam. Modeling turbulent two–phase flows. In *16th Annual Conference on Liquid Atomization and Spray Systems.* ILASS, May 2003.

[3] S. Subramaniam. Properly constrained interphase momentum transfer models for constant-density two-phase flow: resolution of the ill-posedness issue in canonical problems. In *15th Annual Conference on Liquid Atomization and Spray Systems.* ILASS, May 2002.

[4] S. Elghobashi, T. Abou-Arab. A two–equation turbulence model for two–phase flows. *Phys. Fluids*, 26:931–938, 1983.

[5] S. Elghobashi, T. Abou-Arab, M. Rizk, A. Mostafa. Prediction of the particle-laden jet with a two-equation turbulence model. *Int. J. of Multiphase Flow*, 10(6):697–710, Dec. 1984.

[6] A. Mostafa, S. Elghobashi. Two–equation turbulence model for jet flows laden with vaporizing droplets. *Int. J. of Multiphase Flow*, 11(4):515–533, 1985.

[7] G. Ahmadi, D. Ma. A thermodynamical formulation for dispersed multiphase turbulent flows: I basic theory. *Int. J. of Multiphase Flow*, 16(2):323–340, 1990.

[8] D. Ma, G. Ahmadi. A thermodynamical formulation for dispersed multiphase turbulent flows: II simple shear flows for dense mixtures. *Int. J. of Multiphase Flow*, 16(2):341–351, 1990.

[9] J. Cao, G. Ahmadi. Gas–particle two–phase turbulent flow in a vertical duct. *Int. J. of Multiphase Flow*, 21(6):1203–1228, Nov. 1995.

[10] O. Simonin. Continuum modelling of dispersed turbulent two-phase flows part 1: General model description. Technical report, Von Karman Institute of Fluid Dynamics Lecture Series, 1996.

[11] O. Simonin. Continuum modeling of dispersed turbulent two-phase flows part 2: Model predictions and discusstion. Technical report, Von Karman Institute of Fluid Dynamics Lecture Series, 1996.

[12] O. Simonin. Statistical and continuum modeling of turbulent reactive particulate flows. part I: Theoretical derivation of dispersed phase Eulerian modeling from probability density function kinetic equation. Unpublished, 2000.

[13] P. Février, O. Simonin. Statistical and continuum modelling of turbulent reactive particulate flows. part II: Application of a two-phase second-moment transport model for prediction of turbulent gas-particle flows. Unpublished, 2000.

[14] B. Sofiane. Private communication. MFIX mail list, WWW.MFIX.ORG, 2002.

[15] Eduardo J. Bolio, Jules A. Yasuna, J. L. Sinclair. Dilute turbulent gas–solid flow in risers with particle–particle interactions. *AIChE Journal*, 41(6):1375–1388, Jun. 1995.

[16] S. Dasgupta, S. Sundaresan, R. Jackson. Turbulent gas-particle flows in vertical risers. *AIChE Journal*, 40(2), 1994.

[17] M. Syamlal. MFIX documentation user's manual. Technical report, EG&G Technical Services of West Virginia, Inc., U.S. DOE Morgan town Energy Technology Center, Nov. 1994.

[18] T. B. Anderson, R. Jackson. A fluid mechanical description of fluidized beds equations of motion. *I&EC Fundamentals*, 6(4):527–539, Nov. 1967.

[19] H. Enwald, E. Peirano, A. E. Almstedt. Eulerian two-phase flow theory applied to fluidization. *Int. J. of Multiphase Flow*, 22(Suppl.):21–66, 1996.

[20] A. M. Ahmed, S. Elghobashi. On the mechanisms of modifying the structure of turbulent homogeneous shear flows by dispersed particles. *Phys. Fluids*, 12(11):2906–2930, 2000.

[21] D. A. Drew. Mathematical modeling of two-phase flow. *Ann. Rev. Fluid Mech.*, 15:261–291, 1983.

[22] J. R. Fessler, J. D. Kulick, J. K. Eaton. Prefential concentration of heavy particles in a turbulent channel flow. *Phys. Fluids*, 6(11):3742–3749, Nov. 1994.

[23] K. D. Squires, J. K. Eaton. Particle response and turbulence modificaton in isotropic turbulence. *Phys. Fluids A*, 2(7):1191–1203, Jul. 1990.

[24] K. D. Squires, J. K. Eaton. Particle response of particles by turbulence. *Phys. Fluids A*, 3(5):1169–1178, May 1991.

[25] S. B. Pope. *Turbulent flows.* Cambridge University Press, 1999.

[26] G. Balzer, A. Boelle, O. Simonin. Eulerian gas–solid flow modelling of dense fluidized bed. In *Fluidization VIII*, pages 1125–1134. International Symposium of Engineering Foundation, 1998.

[27] D. C. Besnard, F. H. Harlow. Turbulence in two–field incompressible flows. Technical report, LA-10187MS, Los Alamos Lab, Albuquerque, NM, 1985.

[28] M. S. Mohamed, J. C. LaRue. The decay power law in grid-generated turbulence. *J. Fluid Mech.*, 219:195–214, 1990.

[29] J. D. Lambert. *Numerical methods for ordinary differential systems: the initial value problem.* John Wiley & Sons, 1991.

[30] G. M. Pai, S. Subramaniam. Analysis of turbulence models in Lagrangian-Eulerian spray computations. In *In Proceedings of the 17th Annual Conference on Liquid Atomization and Spray Systems.* Intl. Liquid Atomization and Spray System Soc., May 2004.

APPENDIX A. INITIAL VALUES FOR PARTICLE–LADEN ISOTROPIC TURBULENCE

Since the data at the beginning of evolution is contaminated by the setup of the initial conditions in the DNS study for particle–laden isotropic turbulence. The initial conditions all start from $t/T_e = 0.8$ in the thesis. For the different Stokes number, the TKE and dissipation rate in the fluid energy are different. From the DNS study, the total energy of the system is dissipated by two mechanisms:

(1) the viscous dissipation occuring throughout the continuous fluid phase;

(2) losses due to drag at the particle interphase. And particles are significantly dissipative to the total kinetic energy of the system.

In this study, since the model simulation starts from $t/T_e = 0.8$, the initial dissipation rate in fluid phase is chosen to be the sum from the two mechanisms. The initial conditions used in this study are listed in Table. A.1

Table A.1 Initial values of simulation parameters for different particle Stokes numbers

particle Stokes number (St)	$k_f(0)$	$k_p(0)$	$\varepsilon_f(0)$
St=1.6	0.9659	0.8952	0.3627
St=3.2	0.94498	0.8172	0.3996
St=6.4	0.9422	0.8294	0.43835

APPENDIX B. INITIAL VALUES FOR PARTICLE–LADEN HOMOGENEOUS SHEAR FLOWS

In the DNS study for the homogeneous shear flows, the particles are injected in the flow at $T = 1$. All the initial condition presented here is at $T = 1$.

Table B.1 Initial values of parameters common to all the cases for particle–laden homogeneous shear flow

Parameters	Values
ρ_f	1.
ν_f	0.0001050
k_f	0.0014953
k_p	0.0014953

Table B.2 Initial values of parameters for different test cases in particle–laden homogeneous shear flow

Case	τ_p	d	ρ_p/ρ_f	$St = \tau_p/\tau_\eta$	α_p	ϕ_m
B	1.0	1.0×10^{-3}	1890	2.33	5.0×10^{-4}	1.0
C	0.1	6.0×10^{-4}	525	0.233	1.9×10^{-4}	0.1
F	1.0	1.0×10^{-3}	1890	2.33	5.0×10^{-5}	0.1
G	1.0	1.0×10^{-3}	1890	2.33	2.5×10^{-4}	0.5
H	0.5	1.0×10^{-3}	945	1.165	1.0×10^{-4}	0.1
I	0.25	1.0×10^{-3}	472.5	0.583	2.1×10^{-4}	0.1

ACKNOWLEDGEMENTS

I would like to sincerely thank Dr. Subramaniam for his invaluable guidance and encouragement. I also would like to thank my committee members Dr. Battaglia and Dr. Hill, especially for the knowledge gained from Dr. Hill's course (ChemE 652). I also want to express my thanks to people in the CFD lab (0095E) – Anup, Chunjian, Ian, Jay, Jin, John, Joon, Kunlun, Madhu, Nan, Rahul, Ross, Sergiy, Wenny, Xiaofeng and Zhaohui for all their help and nice discussions.

Finally, the love, support and patience of my family and friends is greatly appreciated.

This work was performed at Ames Laboratory under Contract No. W-7405-Eng-82 with U.S. Department of Energy. The United States government has assigned the DOE report number IS-T 2493.